DEMOCRATIC PEOPLE'S REPUBLIC OF ALGERIA
MINISTRY OF HIGHER EDUCATION AND RESEARCH
SCIENTIFIC
MOHAMED BOUDIAF - M'SILA UNIVERSITY

FACULTY OF TECHNOLOGY
DEPARTMENT OF ELECTRICAL ENGINEERING
N° : ELM-05

FIELD: ELECTROMECHANICAL
OPTION: ELECTROMECHANICAL

Thesis submitted for the Academic Master's degree By:

CHIKHI HOSSEM EDDINE

BOUHNIK ISMAIL

THEME

Study of an Autotransformer Superconductor

Supported by the jury composed of:

Pr. GHEMARI ZINE	University of Mohamed Boudiaf M'Sila	President
Pr. BELKHIRI Salah	University of Mohamed Boudiaf M'Sila	Reporter
Dr. DEFDAF Mabrouk	University of Mohamed Boudiaf M'Sila	Examiner
Pr. DJERIOUI Ali	Representative of the incubator/ CATI	Examiner
Mr. YAHIAOUI Slimane	SPE of M'sila	Examiner

AcademicYear:2024/ 2025

Gratitude

With deep humility and gratitude, we first extend our thanks to **Allah, the Almighty**, who granted us health, strength, and perseverance to complete this academic work.

We would also like to express our sincere appreciation to our esteemed supervisor, **Pr. BELKHIRI Salah**, for his valuable guidance, continuous support, and generosity with his time. His insightful remarks and scientific expertise have played a fundamental role in shaping the quality and direction of this research.

Our heartfelt thanks also go to the **respected members of the examination committee** for their time, thoughtful feedback, and for honoring us with their evaluation of our work. Their observations are a source of encouragement and inspiration for our future academic endeavors.

Dedication

All praise is to Allah, Lord of the Worlds, the Guide to all that is right, the One who eases every difficulty. By His grace, good deeds are accomplished, and by His facilitation, great tasks are achieved.

To my beloved parents, my two brothers, my dear sister, and my entire family,
For your inexhaustible patience, unshakable support, and unwavering faith—the greatest motivators of my journey;
To my teachers and advisors, who carried the torch of knowledge to illuminate my path and refined my efforts with their wisdom;
To my friends and colleagues, my steadfast allies in times of need and reminders of purpose in moments of doubt;
And to everyone who contributed to this achievement, even with a word of encouragement or advice—may Allah reward you with the finest recompense.

This work is dedicated first and foremost to Allah, then to those who entrusted me with their confidence and love, becoming my greatest support and inspiration.

Bouhnik ismail

Dedication

To all who believed in me, your faith and encouragement made this journey possible. This achievement is dedicated to you.

Chikhi Hossem Eddine

ملخص

تناولت هذه الدراسة مقارنة بين محول ذاتي تقليدي وآخر مدمج بمواد فائقة التوصيل (YBCO)، من حيث الأداء الكهرومغناطيسي والحراري. باستخدام طريقة العناصر المحدودة عبر MATLAB/PDETOOL ، أظهرت النتائج انخفاض الفاقد الحراري وزيادة كثافة التيار وتحسن الاستقرار الحراري في النموذج الفائق التوصيل، مما يبرز كفاءته في التطبيقات الحديثة.

الكلمات المفتاحية: محول ذاتي، مواد فائقة التوصيل، MATLAB، كثافة التيار.

Résumé

Cette étude compare un autotransformateur classique à un autre intégrant des matériaux supraconducteurs (YBCO). Grâce à la méthode des éléments finis sous MATLAB/PDETOOL, les résultats montrent une réduction des pertes thermiques, une meilleure densité de courant et une stabilité thermique accrue.

Mots-clés : Autotransformateur, Supraconducteurs, MATLAB, Densité de courant.

Abstract

This study compares a conventional autotransformer with one using superconducting materials (YBCO). Finite Element simulations via MATLAB/PDETOOL show reduced thermal losses, higher current density, and improved thermal stability in the superconducting model.

Keywords: Autotransformer, Superconductors, MATLAB, Current Density.

Table of contents

CHAPTER II: Modelling of Superconducting Materials

CHAPITRE III: Application and Results of simulation

List of figures

Chapter I

Chapter II

Chapter III

List of Tables

Chapter I

Chapter III

List of Symbols and Abbreviations

Jc	**Critical current density**	**[A/m2]**
Tc	**Critical temperature**	**[K]**
Hc	**Critical magnetic field**	**[A/m]**
B	**Magnetic induction**	**[T]**
μ_0	**Magnetic permeability of vacuum**	**[H/m]**
H	**Magnetic field**	**[A/m]**
E	**Electric field**	**[V/m]**
B	**Magnetic induction**	**[T]**
D	**Electric induction**	**[C/m2]**
ρ	**Volumetric charge density**	**[C/m3]**
LTS	**Low Temperature Superconductors**	
SMES	**Superconducting Magnetic Energy Storage**	
LCT	**Low critical temperature**	
HCT	**High critical temperature**	
TAFF	**Thermally activated flux-flow**	
S	**Apparent power**	**[kVa]**
f	**Supply frequency**	**[Hz]**
V_{pri}	**Primary voltage**	**[V]**
V_{sec}	**Secondary voltage**	**[V]**
I_{pri}	**Primary current**	**[A]**
I_{sec}	**Secondary current**	**[A]**
T	**Ambient temperature**	**[K]**
T	**Maximum temperature**	**[K]**
h	**Convection coefficient**	

General Introduction

General Introduction

The growing demand for efficient and reliable electrical power transmission, coupled with the rapid advancement of high-power applications, has driven significant improvements in electrical engineering, particularly in the design of transformers and power systems. While traditional electrical transformers effectively step up or down voltage levels, they often experience inefficiencies due to resistive losses, thermal dissipation, and the inherent limitations of copper or aluminum windings. These issues become particularly pronounced in high-voltage, high-current applications, where energy losses can be considerable and the size and weight of transformers can become unwieldy.

Recently, the incorporation of superconducting materials into electrical systems has emerged as a promising solution to these challenges. Superconductivity, which is characterized by the complete absence of electrical resistance below a certain critical temperature, offers a revolutionary approach to power transmission by allowing systems to operate with near-zero losses and significantly enhanced efficiency. When used in conjunction with the principles of the autotransformer a type of transformer that utilizes a single winding for both primary and secondary circuits—superconducting materials can further optimize performance, leading to more compact, energy-efficient, and high-power systems[1-6].

An autotransformer superconducting system (ATS) combines the high-efficiency potential of superconductivity with the space-saving benefits of an autotransformer design. These systems leverage superconducting materials to minimize power losses during transmission and transformation. The autotransformer configuration reduces the current draw on the secondary side, resulting in smaller and more cost-effective transformer units. This hybrid approach offers substantial enhancements in power handling capabilities, thermal management, and overall system efficiency, particularly in applications involving long-distance transmission, renewable energy integration, and electric transportation systems [7-9].

The primary objective of this thesis is to investigate and model a superconducting autotransformer using simulation software while comparing and analyzing the results with those of a conventional autotransformer. In this study, we will replace traditional winding materials with superconducting materials and evaluate the resulting performance enhancements. Our work is organized as follows

- In the first chapter, we provide a detailed overview of superconducting materials to deepen our understanding of the materials used in our research. We will also present a brief history and discuss the key properties that define various types of superconductors, including High-Temperature Superconductors (HTS) such as YBCO and BSCCO, as well as their industrial applications.
- The second chapter focuses on modeling superconducting materials and the mathematical equations that govern the physical phenomena associated with them. We will explore the behavior of these materials using formulations based on electromagnetic equations, enabling the study and analysis of various phenomena through simulation software.

The final chapter is predominantly descriptive, concentrating on the modeling of a superconducting autotransformer prototype using MATLAB. We will begin by analyzing the conventional characteristics and performance of the autotransformer with copper windings. Subsequently, we will replace the copper windings with superconducting windings to investigate the advantages this change offers. To systematically compare the performance of the two proposed structures, we will highlight the improvements achieved through High-Temperature Superconducting (HTS) materials in conventional autotransformers. This analysis will emphasize the enhanced functionalities, improved efficiency, and expanded range of potential applications made possible by superconducting technology in power systems.

In conclusion, we will summarize the key findings of our thesis and discuss future research directions in this

CHAPTER I

General Overview of Superconductors

I.1 Introduction:

Superconductivity is a quantum phenomenon defined by zero electrical resistivity and perfect diamagnetism, known as the Meissner effect, occurring below a critical temperature (Tc). Discovered by Heike Kamerlingh Onnes in 1911, superconductors are divided into two categories: Type I, which completely expels magnetic fields, and Type II, which allows for partial penetration of magnetic fields. **[1]**

The BCS theory, introduced in 1957, elucidates superconductivity through the formation of Cooper pairs, resulting from electron-phonon interactions. Superconductors play a crucial role in various technologies, including MRI machines, Maglev trains, and energy systems, thus contributing significantly to technological progress. This chapter explores the essential properties, classifications, and theoretical foundations of superconductors, emphasizing their scientific and practical importance.

I.2. Historical Background:

Superconductivity is a quantum phenomenon characterized by the complete disappearance of electrical resistance and the expulsion of magnetic fields in certain materials when cooled below a critical temperature. The discovery of this phenomenon in 1911 by Heike Kamerlingh Onnes at the University of Leiden marked a seminal moment in condensed matter physics. By employing liquid helium to attain temperatures near absolute zero, Onnes observed that the electrical resistance of mercury abruptly diminished at 4.2 Kelvin. This landmark finding not only earned him the Nobel Prize in Physics in 1913 but also represented a significant shift in the scientific understanding of material behavior under extreme conditions. **[1]**

The phenomenon was further illuminated in 1933 by the groundbreaking work of Walther Meissner and Robert Ochsenfeld, who discovered the Meissner effect. This effect demonstrated that superconductors actively expel magnetic fields when cooled below their critical temperature, effectively distinguishing superconductors from perfect conductors and emphasizing their unique quantum characteristics**. [2]**

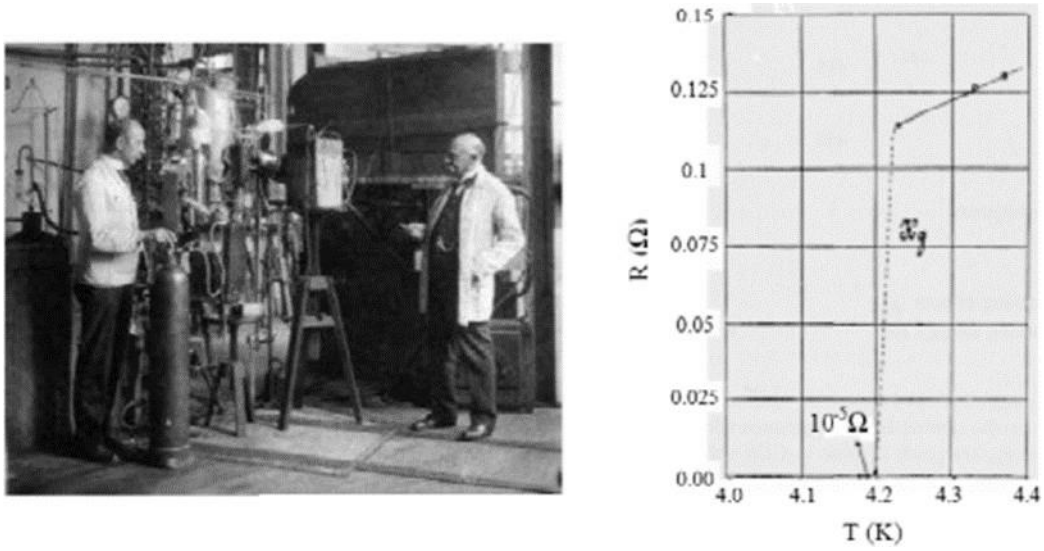

Figure 1.1: Heinke Kammerlingh Onnes - first liquefaction of helium (1908) and discovery of superconductivity (1911) **[3].**

Theoretical frameworks began to evolve in the mid-20th century. In 1950, the Ginzburg-Landau theory, developed by Vitaly Ginzburg and Lev Landau, provided a macroscopic description of superconductivity as a quantum state. This model successfully elucidated various macroscopic properties of superconductors, including magnetic flux quantization. Subsequently, in 1957, a more comprehensive microscopic theory emerged with the BCS (Bardeen-Cooper-Schrieffer) theory. This pivotal work detailed the mechanism by which lattice vibrations mediate electron pairing, culminating in the formation of Cooper pairs that condense into a single quantum state, exhibiting resistance to scattering. Although the BCS theory established a robust framework for understanding conventional superconductors, its applicability was primarily confined to low-temperature phenomena**.[4]**

A significant paradigm shift occurred in 1986 with the discovery of high-temperature superconductivity by Johannes Georg Bednorz and Karl Alexander Müller. Their identification of superconductivity in a lanthanum barium copper oxide compound at 35 Kelvin considerably exceeded the theoretical limitations set by BCS theory. This breakthrough, which garnered the Nobel Prize in Physics in 1987, catalyzed a new chapter in the field and led to the discovery of materials such as YBCO (yttrium barium copper oxide), which superconducts at 92 Kelvin and can be effectively cooled using liquid nitrogen, greatly enhancing the potential for practical applications**.[5]**

Subsequent discoveries, including materials such as BSCCO (bismuth strontium calcium copper oxide) and magnesium diboride (MgB_2), identified in 2001, have further expanded the landscape

of superconductivity research. Notably, MgB_2 serves as a bridge between low and high-temperature superconductors, presenting advantages in cost-effective manufacturing and a spectrum of applications, notably in medical imaging (MRI), power transmission, and transportation technologies, including magnetic levitation (maglev) trains.

Current research endeavors continue to unravel the underlying mechanisms of high-temperature superconductivity, with the overarching objective of achieving room-temperature superconductors. Such advancements possess the potential to revolutionize energy efficiency, transportation systems, and quantum technologies, thereby reaffirming superconductivity's status as a dynamic and continuously evolving frontier in contemporary physics.**[2][3][6-8]**

I.3. Outstanding Features of Superconducting Materials:

I.3.1. No electrical resistance:

The key characteristic of superconducting materials is their complete lack of electrical resistance, a phenomenon first demonstrated by Kamerlingh Onnes. This occurs when the material is cooled below a specific temperature known as the critical temperature. At this point, the resistivity of a superconductor drops suddenly to zero, making it effectively undetectable (see Figure I.2). The temperature range in which this loss of resistivity happens can be quite narrow, sometimes just a few milli-kelvins for certain substances. Exact measurements can reveal resistivity values lower than 10^-25 Ω m**.[4][5][9- 12].**

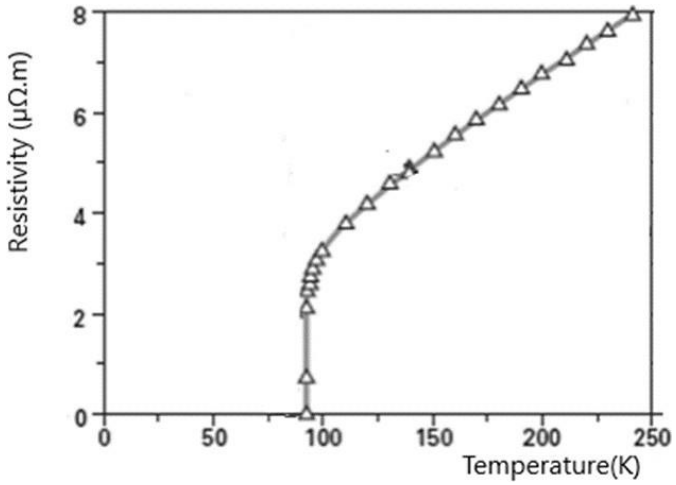

Figure I.2:YBaCuO sample resistivity (A. Sulpice, CNRS-CRTBT)

I.3.2. Meissner Effect:

The secondary characteristic of superconducting materials is their remarkable ability to expel an external magnetic field (Ha) when subjected to temperatures below their critical temperature (Tc). When a superconductor is cooled and then exposed to a weak magnetic field, the magnetic flux lines do not penetrate the material, resulting in a magnetic field (B) inside the superconductor that remains at zero. This phenomenon is known as the Meissner effect.

Meissner and Ochsenfeld demonstrated that a superconductor effectively excludes any external magnetic field when it is below the superconductor's critical field, as illustrated in Figure I.3. Consequently, a superconductor behaves as an ideal diamagnetic material, maintaining a state in which the magnetic field is absent. Further studies indicate that, in the presence of a weak magnetic field, its intensity gradually diminishes at the surface of the superconductor over a depth of approximately 10^-5 cm. When an H-field is applied, a persistent current is induced on the surface of the superconductor to counteract the external field **[13].**

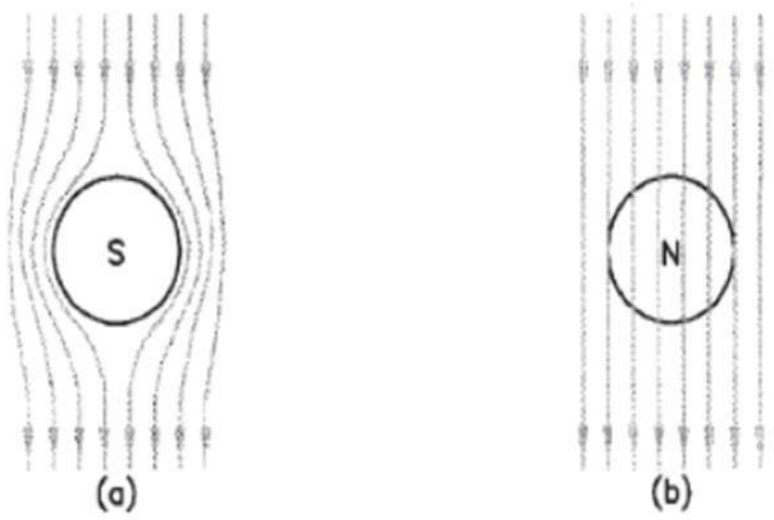

Figure I.3: Field lines around a superconductor. (a) When H <Hc, the system is perfectly diamagnetic and (b) when H >Hc System returns to normal.

I.3.3. The Critical Surface:

The superconducting state is characterized by three essential physical parameters: the critical temperature (Tc), the critical magnetic field (Hc), and the critical current density (Jc). These parameters are significantly interrelated, meaning that the maintenance of the superconducting state requires the magnetic field, current density, and temperature to remain below critical values specific to the material.

In a three-dimensional representation of Figure I.4, the area delineated by these three quantities (Tc, Hc, Jc) is known as the critical surface. Within this surface, the material is in

a superconducting state. The peak values of Hc and Jc are achieved at a temperature of 0 K, whereas the maximum Tc occurs when both the magnetic field and current density are at zero. When the material lies outside this critical surface, it enters either the normal state or the mixed state.**[10].**

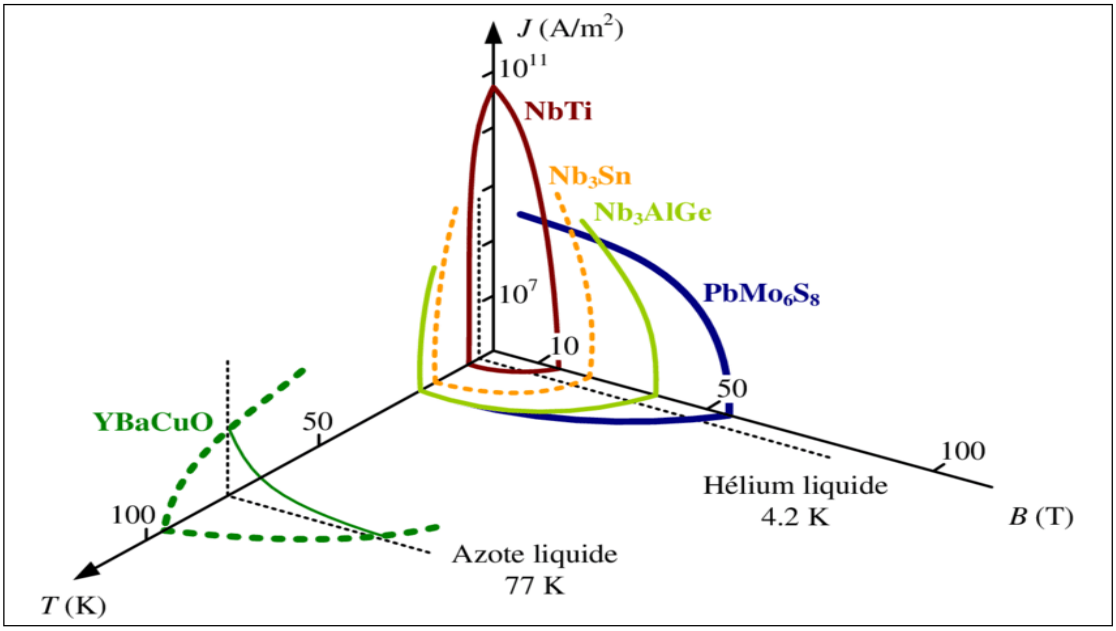

Figure I.4: Critical surface of superconducting materials. **[14]**

I 3.4. BCS Theory:

The first microscopic framework explaining superconductivity, known as BCS theory, was developed in 1957 by John Bardeen, Leon Cooper, and Robert Schrieffer. A fundamental principle of this theory is that electrons near the Fermi level form pairs, termed Cooper pairs, when interacting with the crystal lattice.

This phenomenon is depicted in Figure 1.5: as an electron traverses a conductor, it induces the attraction of positive charges from the nearby lattice structure. This distortion in the lattice creates a region with increased positive charge density, encouraging another electron characterized by opposite spin and energy to migrate into this area. The enhanced positive charge allows the migrating electron to attract an additional electron through lattice vibrations, effectively overcoming Coulomb repulsion and resulting in the formation of bound electron pairs.

These pairs do not remain in a stable state indefinitely; rather, they continuously dissociate and reform. Since isolating individual electrons is impossible, these pairs are considered stable couplings rather than dynamic entities undergoing constant change.

Electron pairs exhibit markedly different behavior compared to solitary electrons. As fermions, they adhere to the Pauli exclusion principle, which states that no two fermions can occupy the

same quantum state simultaneously. However, similar to bosons, these pairs can condense into a single energy level. In a superconductor, where numerous pairs coexist, they form a highly collective condensate, and the energy of this condensate is significantly lower than that of the first excited state**.[15]**

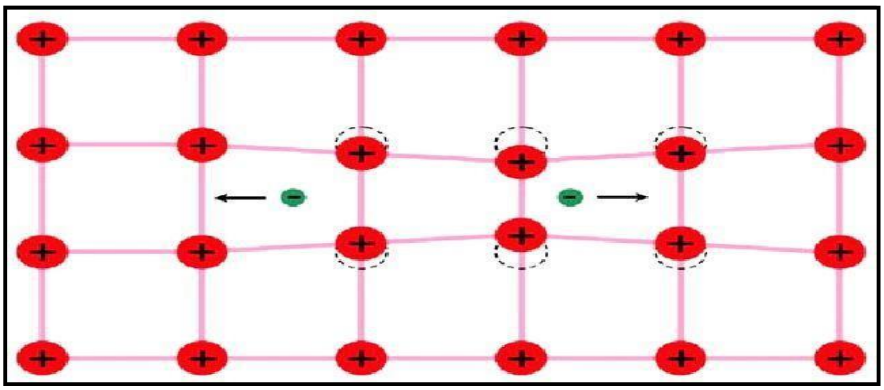

Figure I.5: The formation of a copper pair: an electron passing through attracts positively charged ions from the lattice, causing a slight ripple in its wake. Another electron passing in the opposite direction is attracted by this displacement. **[15]**

The BCS theory, based on the observed isotopic effect in superconducting materials, posits that the critical temperature is inversely related to the mass of the isotope present in the material. This isotopic effect has been documented in numerous superconductors. The theory makes two primary predictions: the superconducting transition temperature (Tc) and the energy gap, particularly in the low coupling regime.**[15]**

I 3.5. Critical Temperature:

Critical temperature, denoted (Tc), is the temperature threshold at which the electrical resistance begins to drop to zero, indicating the beginning of superconductivity in a given material. Superconductivity is basically characterized by the total absence of electrical resistance when the temperature drops below this critical threshold. Essentially, superconducting materials exhibit a loss of resistivity under specific conditions such as temperature, magnetic field strength, and electrical current. Therefore, the electric current is able to pass through a superconducting material without any energy dissipation as long as its thermal state is maintained below the critical temperature **[16].** Figure I.6 shows the relationship between the resistance of a superconductor (especially mercury) and temperature variations.

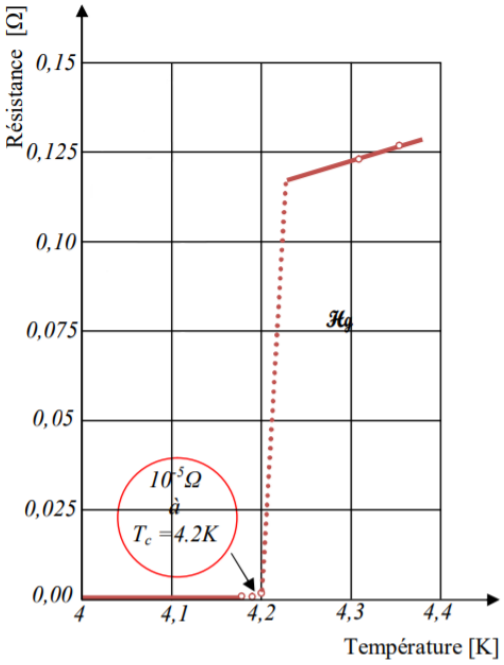

Figure I.6: Temperature-dependent resistance of mercury.

I 3.6. Critical Magnetic Field:

The amplitude of the magnetic field is a crucial parameter in the phenomenon of superconductivity. When the intensity of the magnetic field exceeds a certain threshold,

superconducting materials lose their superconducting properties and revert to a normal conductive state. Superconductors can be classified into two main categories: Type I and Type II superconductors.

Type I superconductors have a specific critical magnetic field value, denoted as Hc. Below this critical value, these materials exhibit superconducting behavior and completely expel magnetic fields from their interior, a phenomenon known as perfect diamagnetism or the Meissner effect. When the magnetic field exceeds this critical threshold, the material transitions back to a non-superconducting state.**[17]**

In contrast, Type II superconductors are characterized by two distinct critical magnetic field values, Hc1 and Hc2. The magnetic induction in the material can be expressed by the following relation:

$B = \mu 0 (H+M)$ **[I.2]**

μ0: Magnetic permeability of the vacuum.

H: The magnetic field inside the material.

M: Magnetization

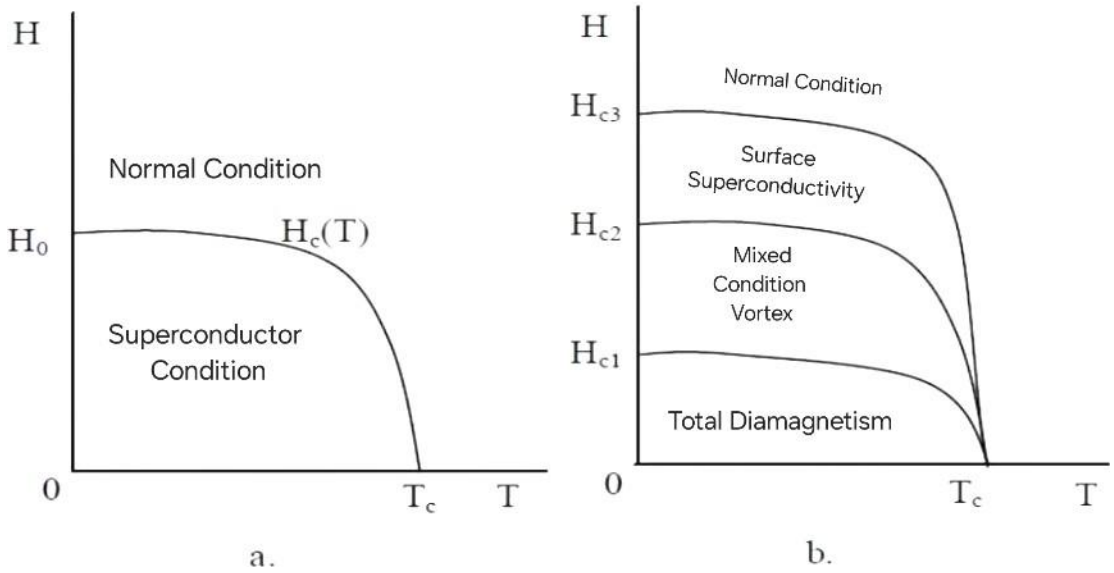

Figure I.7: Representation of the superconductivity types according to field.

I.3.7. Critical Current Density Jc(H,T):

The critical current density represents the maximum permissible value at which an electric field begins to emerge.

In type I superconductors, the distribution of current is non-uniform. The transport current is restricted to the flux at the surface, governed by a parameter known as the London penetration depth.

In contrast, type II superconductors experience a significant impact on their critical current density due to magnetic induction and the presence of vortices within their structure. Under conditions of transverse magnetic induction in the mixed state, an ideal superconductor maintains a zero current density. However, the transport current interacts with these vortices, which begin to move when the generated Lorentz force (JcB) exceeds the anchoring forces.

This results in energy dissipation within the material. When the current density surpasses a critical threshold, denoted as Jc, the vortices are expelled, marking the transition to a state of flux (see Fig. I.8). Once released, the vortices move, creating an electric field that is directly proportional to the difference between the current density and the critical current density (J - Jc). In this flux regime, resistivity dependent on magnetic induction emerges. To achieve high critical current densities, it is crucial that the vortices remain firmly anchored within the material.

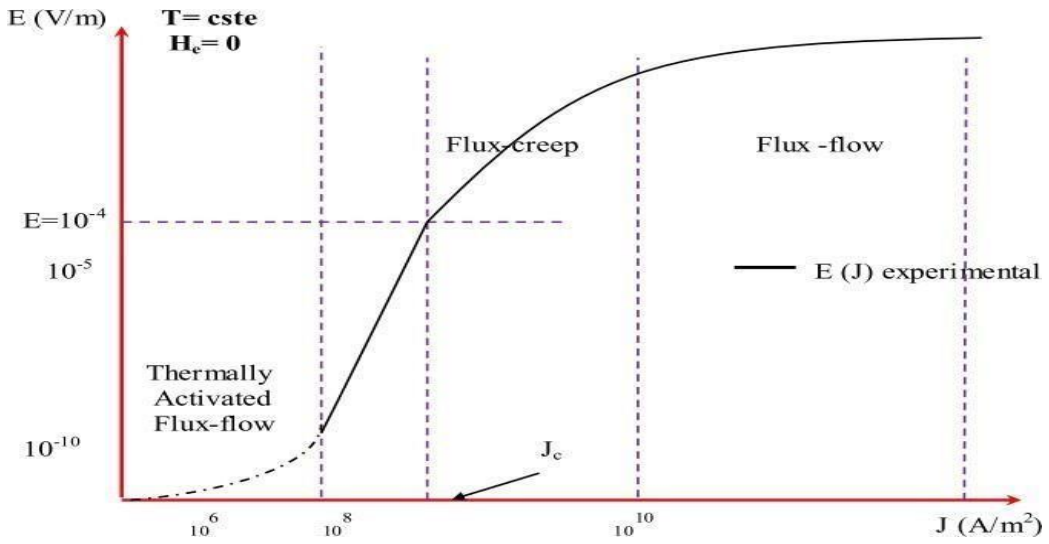

Figure I.8: Dependence of the magnetic field on temperature,**[18].**

I.4. Types of Superconductors:

Superconducting materials are classified into two categories based on their critical magnetic field (Hc): Type I superconductors and Type II superconductors.

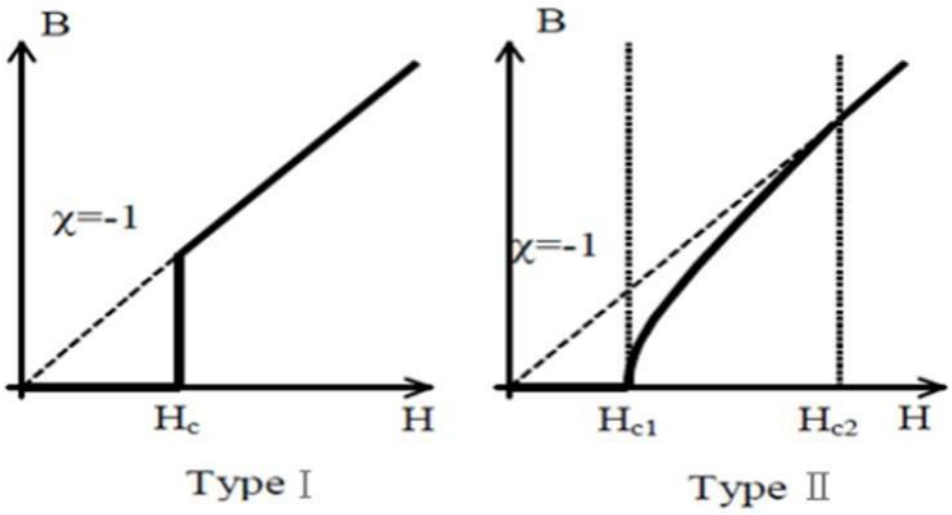

Figure I.9: Magnetic induction as a function of the magnetic field, ideal superconductors of types I and II

I.4.1. Superconductors Type I :

Type I superconductors have a specific critical magnetic field known as Hc. In these materials, the magnetic field penetrates to a certain depth, referred to as the London penetration depth, where supercurrents are generated. The characteristics of this category are relatively straightforward, as they exhibit only two distinct phases: the normal phase, marked by significant resistance, and the superconducting phase, characterized by nearly perfect diamagnetism.

Type I superconductors primarily consist of pure elements, including lead (Pb), mercury (Hg), indium (In), and tin (Sn). The critical magnetic fields associated with these pure elements, which are classified as Type I superconductors, are generally modest and typically do not exceed 0.2 Tesla.**[19-20].**

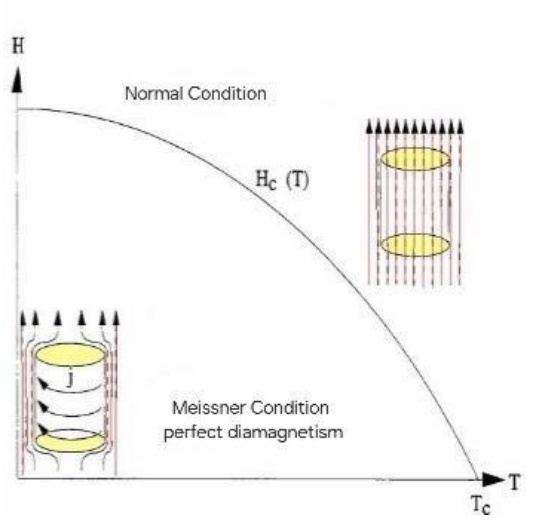

Figure I.10: Phase diagram of a type I superconductor.

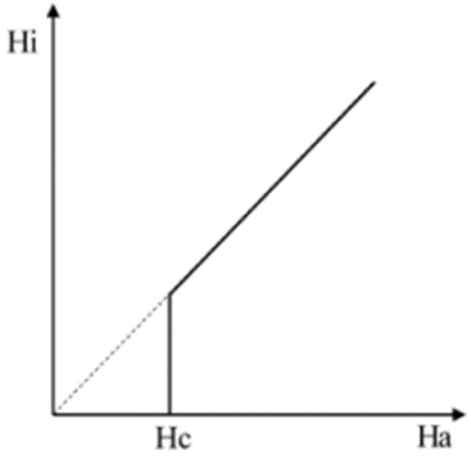

Figure I.11: Magnetic field induced by the applied magnetic field of type I superconductors.

I.4.2. Superconductors Type II:

Type II superconductors are distinguished by their two critical magnetic fields, Hc1 and Hc2, in contrast to Type I superconductors, which possess only a single critical field (Hc). While a few elemental superconductors, such as vanadium, technetium, and niobium, belong to the Type I category, Type II superconductors are predominantly composed of metallic compounds and alloys. This distinction was made in the 1930s, following the discovery of superconductivity in alloyed materials.

When operating below their critical temperature (Tc), Type II superconductors exhibit unique magnetic properties, with significant differences in their induction and magnetization behavior compared to pure metallic superconductors. Importantly.

the second critical field, Hc2, is considerably higher than Hc1, often reaching values in the range of tens of teslas. Furthermore, Type II superconductors demonstrate superior critical values for magnetic fields, temperatures, and current densities compared to their Type I counterparts, making them particularly well-suited for demanding practical applications in advanced electrical engineering and magnet-based systems.

The response of Type II superconductors to an external magnetic field can be categorized into three distinct regions, as illustrated in the accompanying figure I.12.

1. **Region 1: Superconducting State (Meissner State):**

In this phase, when magnetic fields are below Hc1, the material exhibits perfect diamagnetism, entirely expelling the external magnetic field. This phenomenon is analogous to the Meissner effect observed in Type I superconductors.

2. **Region 2: Mixed State:**

When the magnetic field falls between Hc1 and Hc2, the material enters a mixed or vortex state. In this state, the external magnetic field partially penetrates the superconductor in the form of quantized magnetic flux lines known as vortices, while the remaining portions of the material retain their superconducting properties.

3. **Region 3: Normal State:**

Once the magnetic field exceeds Hc2, superconductivity is completely suppressed, resulting in a transition to the normal state, which is characterized by significant electrical resistance.

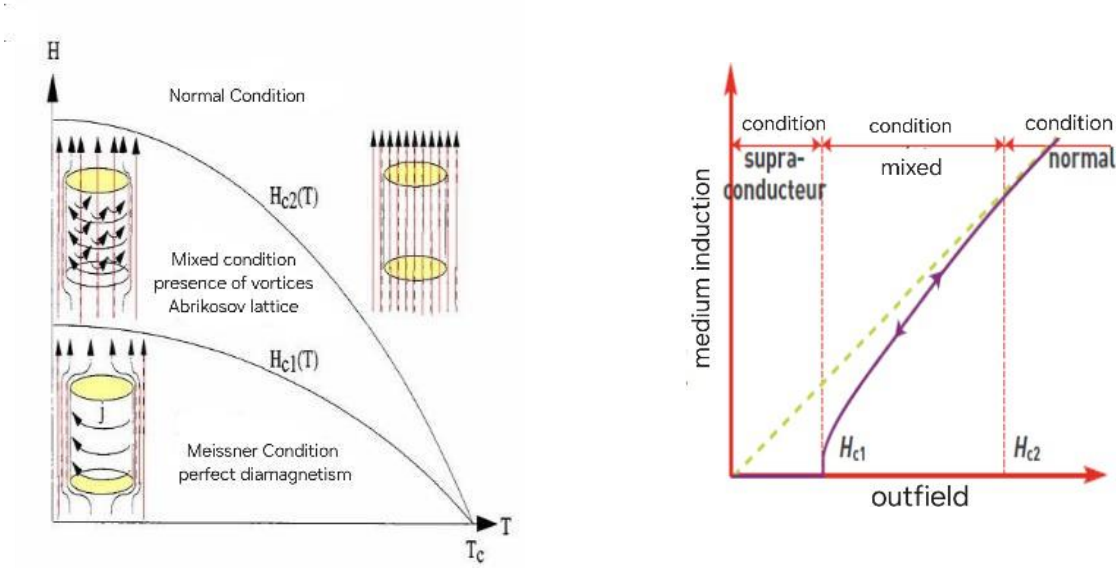

Figure I.12: a - Phase diagram of a type II b superconductor - the characteristic B(H).

The capability of Type II superconductors to function effectively in high magnetic fields, elevated temperatures, and substantial current densities renders them essential for various advanced technological applications. These include high-field magnets, power transmission systems, and state-of-the-art scientific instruments. Consequently, Type II superconductors serve as a fundamental pillar of modern superconducting technologies, especially in scenarios where the performance of Type I superconductors is constrained**.[21-23]**

I.5. Superconducting Materials Categorized by Their Critical Temperature:

I.5.1. Low-Temperature Superconductors (SLCT):

Low-temperature superconductors are the first category of superconductors employed in practical applications, classified as Type I superconductors. They have critical temperatures below 20 K, which necessitates the use of liquid helium for their operation. Commonly utilized materials include NbTi and Nb3Sn, known for their excellent ductility, allowing for the fabrication of coils that can withstand strong magnetic fields. These superconductors have extensive applications in medical imaging devices, with wire lengths extending to several kilometers. Moreover, the durability of these metallic alloys makes them easy to handle and enables remarkable bending radii **[24].**

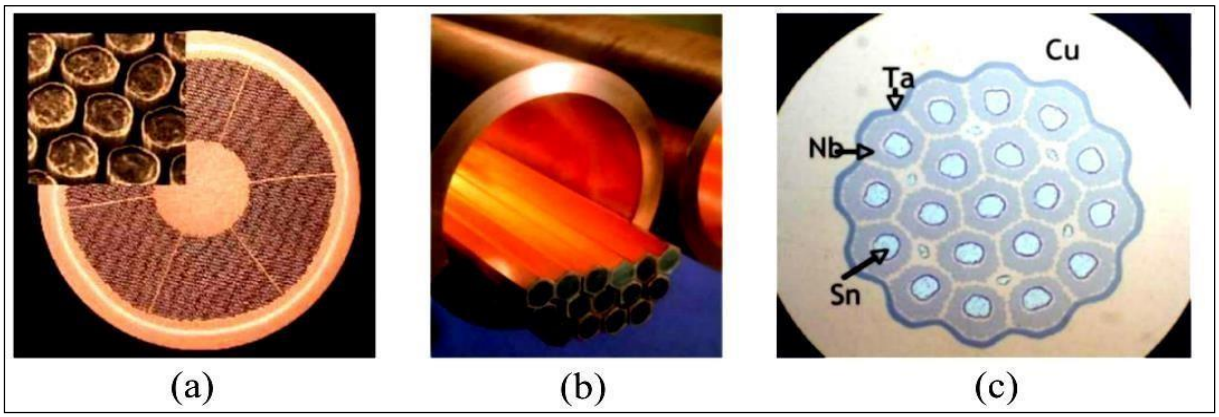

Figure I.13: (a) NbTi wire finalized, (b) bar assembly before wire drawing, (c) Nb3Sn wire before heat treatment **[24-25].**

Table I.1 gives some examples of the critical low temperature superconducting materials, as well as their critical temperatures.

Supraconducteur	T_C(K)
Nb-Ti	9
Nb_3Sn	18
Nb_3Al	19
Nb_3Ga	20

Table I.1: Low Temperature Superconductors (SLCT).

I.5.2. High-Temperature Superconductors (SHCT):

The advent of high-temperature superconductors in 1986 represented a remarkable breakthrough, primarily utilizing ceramic compounds like barium and yttrium. This category is categorized into two main types: BSCCO and YBCO. BSCCO features a Powder Tube (PIT) structural configuration, which renders it a robust wire ideal for coil manufacturing in applications such as electric motors, with cable lengths reaching up to 1,000 meters. On the other hand, YBCO is distinguished by its multilayer structure, derived from sintered and annealed materials, and operates effectively at high current densities and enhanced magnetic fields, with available lengths approaching 500 meters. This type is predominantly employed in power transmission lines.

Current research emphasizes YBCO, alongside investigations into bulk materials composed of single domains that can endure exceptionally high magnetic fluxes. This advancement paves the way for designing magnetic shields or trapped magnetic fields for superconducting magnet development. Presently, discs with diameters of up to 50 mm can be manufactured, featuring rectangular or even hexagonal shapes. **[26] [14].**

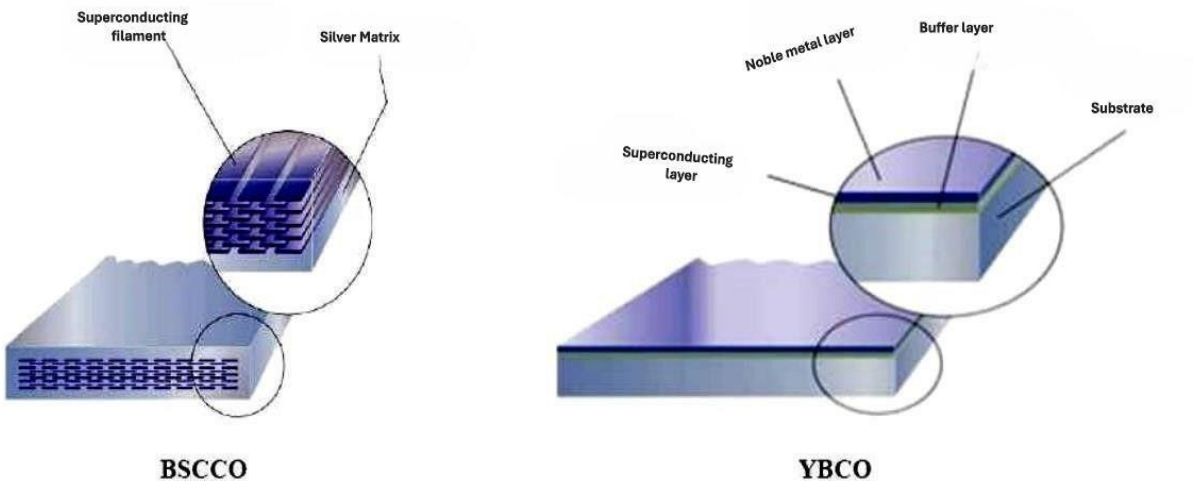

Figure I.14: HTC superconducting wires**[9].**

Supraconducteur	**T_C(K)**
$La_{1.85}Ba_{0.15}CuO4$	35
$La_{1.85}Sr_{0.5}CuO_4$	40
$YBa_2Cu_3O_7$	95
$Bi_2Sr_2CaCu_2O_8$	85
$Bi_2Sr_2Ca_2Cu_3O_{10}$	110
$Tl_2Ba_2CaCu_2O_8$	108
$Tl_2Ba_2Ca_2Cu_2O_{10}$	125
$HgBa_2Ca_2Cu_3O_{6+5}$	133.5

Table I.2: High Critical Temperature Superconductors (HTS).

Table I.2 gives some examples of the critical high temperature superconducting materials, as well as their critical temperatures.

I.6. High-Temperature Superconductor Types :

High-temperature superconductors (HTS) are composed of compounds characterized by repetitive arrangements of various atoms and elemental units, commonly known as unit cells. One example of a superconducting unit cell is HTS-Bi2Sr2Ca2Cu3Ox. These materials appear as tiny crystals consisting of billions of unit cells, often described as beads. The fabrication of macroscopic samples necessitates the aggregation of millions of these particles. HTS materials are inherently fragile ceramics, primarily composed of oxides, and they exhibit tensile strengths approximately 100 times greater than that of copper at room temperature.

The groundbreaking discovery of high-temperature superconductors was made by Bednorz and Müller, who identified lanthanum barium copper oxide ((La, Ba)2CuO4) with a critical temperature (Tc) slightly above 30 K. The highest critical temperature recorded to date is 134 K for HgBa2Ca2Cu3O8. The first superconductor to exceed a Tc of 77 K was yttrium barium copper oxide (YBa2Cu3Ox), commonly referred to as YBCO or Y-123.

	YBCO	Bi-2212	Bi-2223
T_c(K)	93	78	110
B_{irr}4.7K(T)	>30	>30	>30
B_{irr}77K(T)	>5	0.005	0.5
J_c4.7K(A/mm^2)	>100,000	5,000	3,000
J_c77K(A/mm^2)	>10,000	100	500

Table I.3: Critical parameters of HTS superconductors for power applications **[28].**

Alongside bismuth oxides Bi2Sr2CaCu2Ox and Bi2Sr2Ca2Cu3Ox, which are now known as Bi-2212 and Bi-2223 HTS, respectively, these materials represent some of the most advanced in this field. Collectively, Bi-2212 and Bi-2223 are referred to as BSCCO, an acronym for bismuth, strontium, calcium, and copper oxides. Figures 1 to 3 present the key parameters for YBCO, Bi-2212, and Bi-2223, which are the most commonly utilized high-temperature superconductors. **[26] [27].**

Figure I.15: Different forms of SHTC: a) YBaCuO block, b) YBaCuO single layer, c) BSCCO tubes.

I.6.1. Superconductor BSCCO:

BSCCO connectors serve as the fundamental components for all major high-temperature superconducting (HTS) applications and are recognized as first-generation prototypes. Both BSCCO and commercially available connectors can be manufactured in extended lengths of up to 1 kilometer. These connectors are utilized in contemporary transmission systems and are produced using the oxide powder in a tube (OPIT) method.

In a BSCCO conductor, electric current must pass through the grain joints, which restricts the flux from all angles except for minimal directions. Therefore, achieving a robust texture is essential. The alignment of grains is directly related to the increase in critical conductor current density. To ensure the desired texture and orientation of the grains, originally randomly distributed in the oxide powders, a rolling process is employed during manufacturing. This process results in

the formation of superconductors in thin strips that are typically 2 to 4 mm wide and 0.2 to 0.4 mm thick.

HTS compounds are inherently fragile materials. To significantly enhance the mechanical properties of the tapes, the superconducting material is wrapped in a silver (Ag) tube, chosen for its mechanical strength and excellent oxygen diffusion capabilities. The ribbons may contain a single-filament or multifilament BSCCO core. **[28]**

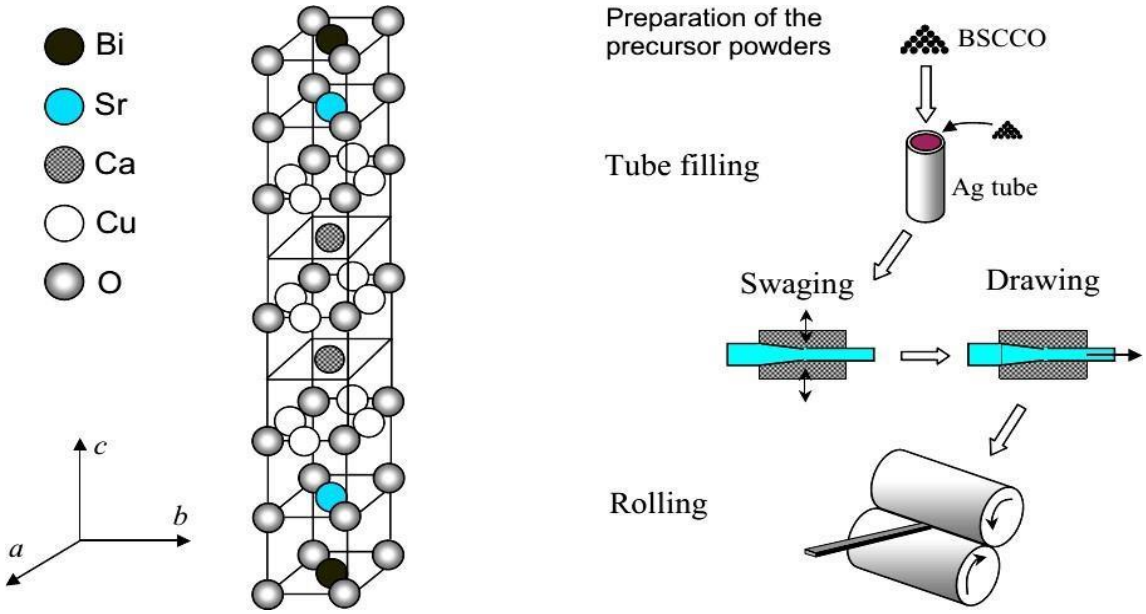

Figure I.16: Bi2Sr2Ca2Cu3Ox unit cell and schematic presentation of the OPIT Technique. Intermediate and final heat treatment is not indicated. **[28]**

BSCCO is characterized by the intrinsic variability of its single-layered, single-cell structure across the a, b, and c crystallographic planes, alongside the anisotropic behavior of the tapes produced due to their stratification during manufacturing. One important characteristic of BSCCO materials is the notable variation in critical current density (Jc). When a magnetic field is applied perpendicular to the tape edge (B//CB), Jc drops sharply; however, under a parallel magnetic field (B//a, b), Jc experiences a more gradual decrease. For simulation purposes, the anisotropic nature of Jc in Bi-2223 tapes is analyzed.

BSCCO features a Bi-O bilayer that approaches an insulating state, making it suitable for superconductor-insulator-superconductor configurations in electronic applications. The irreversibility field at 4.2 K is crucial for both Bi-2212 and Bi-2223. Notably, the critical current density of Bi-2223 decreases more rapidly when subjected to an applied field than that of Bi-2212. At 4.2 K, Bi-2212 can sustain current densities of up to 1000 A/mm² in a magnetic field of 26 T, while Bi-2223 exhibits comparatively reduced current density.

As a result, Bi-2212 is preferred for applications involving high-temperature superconducting magnets that operate at 4.2 K and above 20 K, despite experiencing significant performance degradation due to extreme flux creep and an irreversibility field of only 0.005 T at 77 K. Conversely, Bi-2223 at 77 K shows an irreversibility field of 0.5 T, which, while not critical for magnet design, is advantageous for direct current (DC) applications. Consequently, Bi-2223 has become the predominant material for wire and cable applications at 77 K.**[29].**

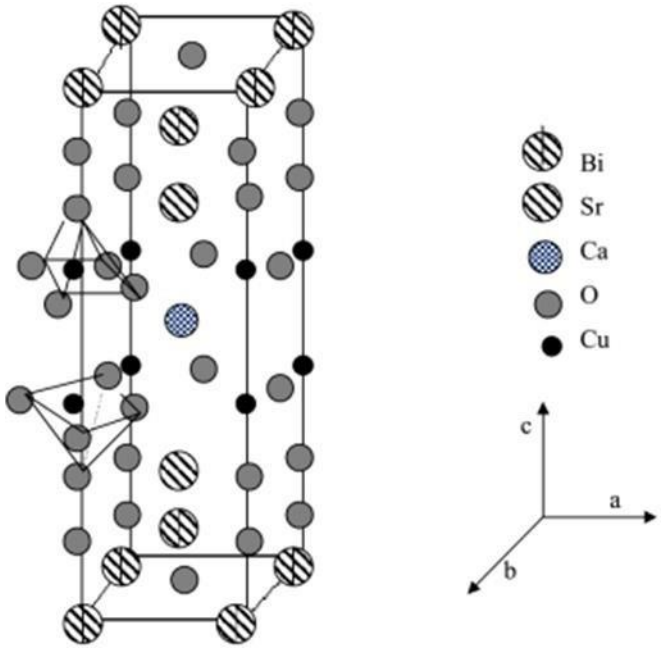

Figure I.17: Crystallographic structure of Bi2Sr2CaCu2O8. **[29]**

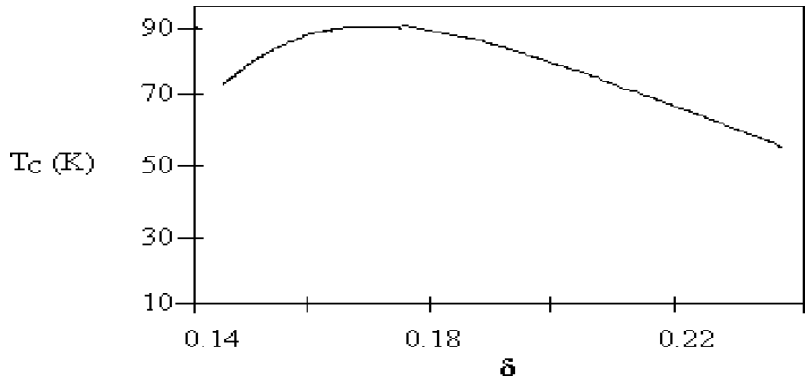

Figure I.18: Critical temperature variation as a function of d in Bi2Sr2CaCu2O7+d. **[29]**

I.6.2. Superconductor YBCO:

One of the primary differences between BSCCO and YBCO lies in their fundamental structures. The YBCO reservoir layer features a metallic composition that is not insulated, in contrast to the insulating nature of BSCCO. Consequently, YBCO exhibits a lower variance. This material achieves remarkably high current densities, exceeding 10,000 A/mm² at a temperature of 77 K. However, producing long lengths of YBCO presents challenges due to manufacturing processes that differ significantly from those employed for BSCCO.

BSCCO used as a coated conductor consists of a thin layer of high-temperature superconductor (HTS) only a few micrometers thick, which is deposited on a flexible substrate. A specific technique used in this context is ion beam-assisted deposition (IBAD). This method involves the deposition of HTS wires onto an aligned insulating layer (the IBAD layer) located on a flexible substrate, aimed at enhancing the orientation of the HTS wires and optimizing their electrical performance. Additional challenges arise from the use of reinforced composite substrates (RABIT) and inclined substrate deposition (ISD), with YBCO being recognized as the most suitable material for second-generation conductors. Nonetheless, the large-scale production of YBCO remains unfeasible, prompting researchers to invest significant efforts into addressing this issue.**[28]**

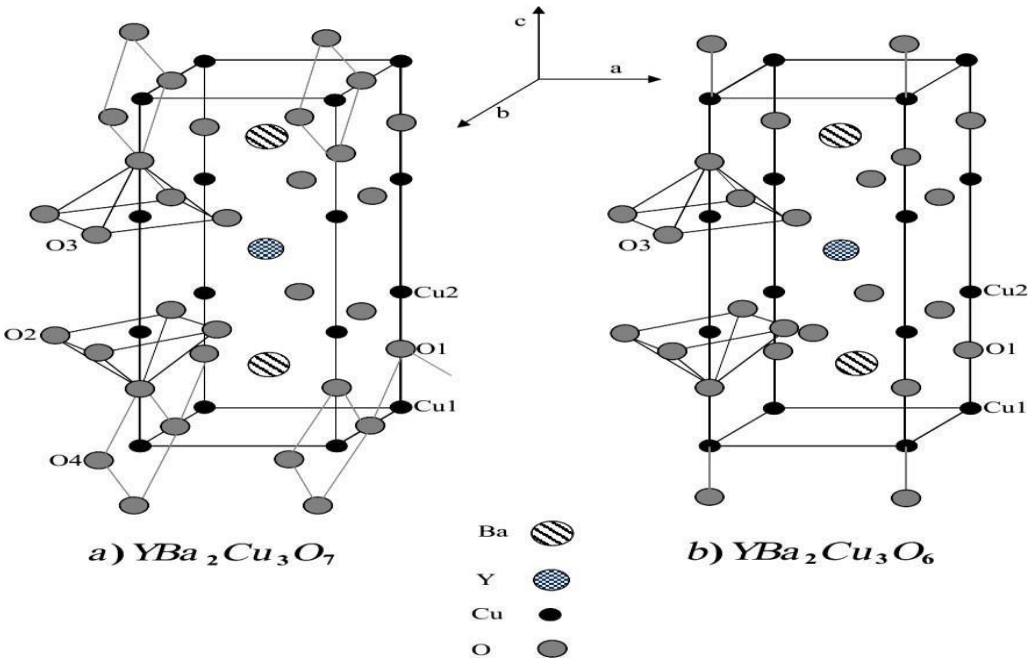

Figure I.19: Crystallographic structure of YBa2Cu3Oy. a) Orthorhombic structure. b) Tetragonal structure. **[29]**

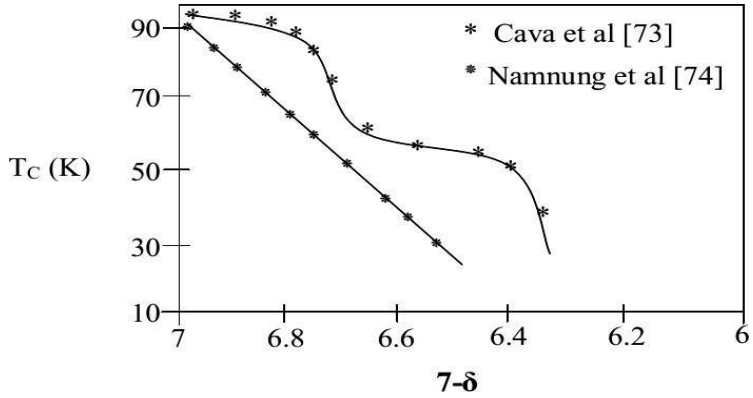

Figure I.20: Critical temperature variation as a function of (7-d) in YBa2Cu3O7-d **[29].**

I. 7. Main applications of superconductors:

Superconducting applications in electrical engineering can be classified into three distinct categories, each based on the advantageous properties of magnetic induction produced by superconductors:

1. Extremely Intense Magnetic Fields: This category pertains to field coils and energy storage systems.
2. Robust Magnetic Fields This classification encompasses motors, generators, transformers, and energy storage systems.
3. Minimum Magnetic Fields: This classification relates to power lines, transformers, and current limiters.**[30].**

I. 7.1. Rotating machines:

Superconductors are commonly employed in rotating machines across various industries due to their ability to enhance operational efficiency. The incorporation of superconductors in chillers has resulted in the creation of several prototypes. By substituting copper windings with superconducting windings, these machines can achieve higher mass due to increased wire current densities and improved magnetic circuit performance.

The substantial mass torque generated by these machines presents a compelling application for embedded systems. **[13]**

I.7.2. Superconducting permanent magnets:

A large superconductor can function as a permanent magnet. By cooling a superconductor at a high critical temperature to a state of zero magnetic field and then rapidly altering the external magnetic field, it effectively encapsulates that magnetic field. The magnetic field retained within

the superconductor is linked to the currents generated according to Lenz's law. These currents resemble those found in conventional conductive materials, originating from the outer surface; however, unlike resistive materials, they do not exhibit any attenuation due to the absence of electrical resistivity. As the external magnetic field diminishes, the configuration of currents adjusts to counter this new fluctuation, facilitating the trapping of induction. For the superconductor to successfully capture the magnetic field, it is crucial that the external field reaches a specific threshold known as the HP penetration field. **[31]**

I.7.3. Transport cables:

The energy losses associated with superconductors are considerably lower than those found in conventional cables, making them especially beneficial for power transmission applications. However, the challenges posed by cryogenics remain intricate and demand long-term solutions. One proposed approach involves circulating coolant through a tube situated at the center of the cable, around which the superconducting wire is wound. As energy demands continue to rise, there is a need to strengthen certain power lines; however, space constraints often limit the installation of new cables. This situation makes superconductors a viable alternative**.[13]**

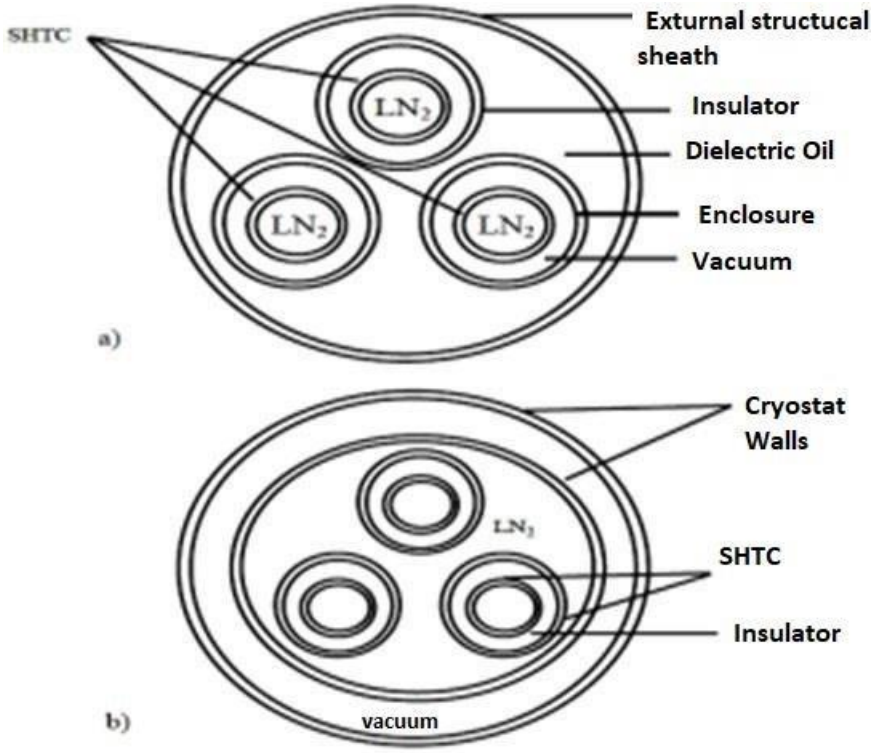

Figure I.21: Schematic representation of a three-phase high-voltage superconductor cable Critical temperature (SHTC) cooled with liquid nitrogen (LN2):

(a) Each phase is situated within a cryogenic chamber, while the insulation is maintained at room temperature.

(b) A single cryogenic chamber accommodates all three phases, with each phase consisting of

two concentric conductors, and the insulation kept at a lower temperature.

I.7.4. Energy storage:

This technological advancement focuses on the storage of energy in the form of a magnetic field, generated by the flux of electric current within a superconducting coil that is short-circuited and maintained at its critical temperature. These coils are known as SMES, or "superconducting magnetic energy storage" systems. As a result, the current flows through these coils without any energy dissipation, enabling a specific amount of energy to be stored for a theoretically indefinite duration. **[13]**.

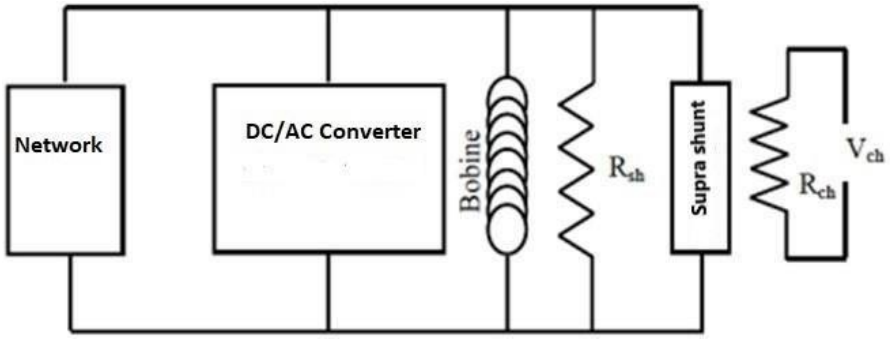

Figure I.22: Schematic of a superconducting coil coupled to a network electrical via a converter; Rsh is the protection resistance; Rch and Vch form the heating circuit of the superconducting shunt. **[32-33]**

Figure I.23: Conductor formed of 4 superconducting tapes isolated from each other**[32-33].**

I.7.5. Autotransformers:

Autotransformers, which utilize a single winding for both primary and secondary functions, play a vital role in regulating electrical voltage. The incorporation of superconducting materials into these devices presents promising opportunities to improve efficiency and minimize energy losses. A significant study explored the fabrication and testing of a superconducting air-core autotransformer rated at 2.5 kVA, revealing enhanced performance when compared to conventional autotransformers**. [34-35]**

The advantages of employing superconductivity in autotransformers include substantial reductions in Joule losses, improved thermal management, and increased power density. Nevertheless, several challenges persist, particularly regarding design optimization, operational stability, and the high costs associated with superconducting materials. Ongoing research is essential to refine these technologies and make them feasible for large-scale application.

I.7.6. Current limiters:

Superconducting current limiters are a category of non-linear circuit components specifically designed to protect electrical systems, such as doors, in the event of a malfunction. Recently, a new generation of superconducting limiters has been developed. The operation of any superconducting system necessitates cryogenic adjustment, which typically involves the use of a cryostat along with cryogenic fluid or a cryogenator. The underlying principle of superconducting current limiters is their transition from the superconducting phase to the normal phase when the electrical current surpasses a critical threshold (Ic). This transformation must occur within a very short time frame to effectively limit the initial overvoltage to a maximum value not exceeding three to five times the rated current.**[36]**

I.8.Conclusion:

In this chapter, we have carefully presented a comprehensive study on the captivating field of superconducting materials, an important area of research within condensed matter physics. It is crucial to acknowledge that superconductors can be classified into two distinct categories: Type I and Type II, each exhibiting unique characteristics and behaviors that merit further investigation. These materials are defined by a specific set of critical physical parameters, including critical temperature (denoted as Tc), critical magnetic field (Hc), and critical current density (Jc), all of which are fundamental in determining their operational capabilities.

Superconductors, particularly high-temperature varieties, possess exceptional physical properties that pave the way for a vast array of potential applications across various industrial and technological domains. They are especially promising candidates for applications related to electromagnetism, rendering them invaluable in the fields of electrical engineering and electronics. To optimize and enhance the performance of devices utilizing these superconducting materials, a thorough and nuanced understanding of their complex electromagnetic behavior and interactions is essential.

Furthermore, superconducting materials boast a wide range of applications within the expansive domain of electrical engineering, underscoring their versatility and significance in modern technological advancements. In this chapter, we have outlined the most common and promising applications of superconductors, emphasizing their transformative influence on diverse

engineering practices. The following chapter will explore the intricate modeling of these advanced materials, offering vital insights necessary to harness their full potential in real-world applications**.**

CHAPTER II

Modelling of Superconducting Materials

II.1. Introduction:

In the context of the electromagnetic paradigm, physical phenomena are often articulated through partial differential equations (PDEs), which may sometimes exhibit nonlinearity and complexities that hinder their resolution. The thermal model is based on the heat transfer equation, which must incorporate the conditions of interaction with the surrounding medium.

Under specific simplifying assumptions, these equations can be reformulated into ordinary differential equations, which can then be solved analytically. However, for more complex scenarios, like those examined in this study (including boundary conditions, complex geometries, and less restrictive assumptions), these equations become analytically unsolvable.

As a result, we resort to approximation methodologies (numerical) to transform the established partial differential equations into a system of algebraic equations that can be solved computationally. In this chapter, we will define the mathematical formulations that characterize the spatiotemporal evolution of the electromagnetic field in superconducting materials, as well as the behavioral laws that govern them.

II.2. State of the Art:

In the previous chapter, we thoroughly examined the behavior of high-critical-temperature superconductors (HCTS), elucidating a pronounced correlation between various characteristics. HCTSs operate in multiple distinct regimes, which makes identifying an analytical model capable of encompassing all these regimes particularly challenging, especially in the context of two-dimensional or three-dimensional scenarios. Despite this challenge, several models have been designed to represent the superconducting state under specific conditions, based on particular assumptions. The predominant macroscopic model used is the critical state model, commonly referred to as the Bean model, albeit in its simplified form.

These models exhibit considerable fidelity to physical reality and facilitate analytical calculations for simple geometries. Regarding the relationship between Jc and magnetic induction, Kim or exponential models can be used when the superconductor operates near its critical current density.

II.3. Mathematical Equations Governing the Physical Phenomenon

II.3.1. Relation B(H):

The following expression defines the magnetic induction B within the material as a function of the external field H and magnetization M:

$$B=\mu_0 H+ \mu_0 M= (1+x)\ \mu_0 H = \mu_0 \mu r H+\mu_0 M \qquad (II.1)$$

It has been established that superconductors exhibit diamagnetic properties, indicating that when the material is in equilibrium, $H<Hc_1$, B within the material is zero. In other words, M = $-H$ and x= -1. However, when the magnetic field Hc_1 exceeds the critical value H, the superconducting material loses its diamagnetic properties. Due to the relatively low critical field associated with type-II superconductors, the magnetic induction B experienced during their operating phase is generally higher than μ_0Therefore, at the macroscopic level, it can be considered non-magnetic.

Thus, we can express $\vec{(B)} = \mu_0 \vec{(H)}$ (Figure II.1), **[37]**

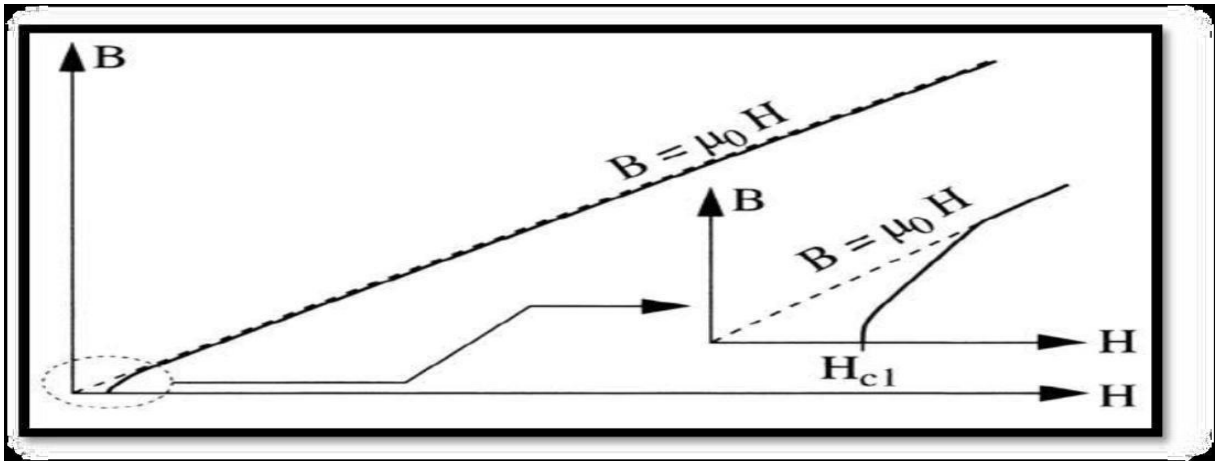

Figure II.1: B(H)Characteristic of a Superconductor **[37].**

II.3.2. Relation E(*J*):

By analyzing the current-voltage characteristics of the sample, it is possible to extrapolate empirical properties V (I), which are often represented in the form of a power law. Assuming this property remains applicable to the current density, the relationship E(J) can be expressed as:

$$E = Ec(J/Jc)^{n} \qquad (II.2)$$

In the context of Equation (II.2), the exponent "n" depends on the specific material, temperature, and magnetic induction. A sharper transition is observed when the index n is high, as illustrated in (Figure II.2).

Sometimes, the amplitude of the superconducting band is considered a metric for evaluating the quality of the superconducting band. An increase in its value indicates an improvement in the material's quality. Indeed, in this scenario, the critical current can be determined with precision as soon as a voltage appears across the sample.

The resolution of Equation (II.2) can be performed using computational software to determine electromagnetic parameters. However, from an analytical perspective, its application becomes challenging, except in cases where the value of « n » is significant **[38].**

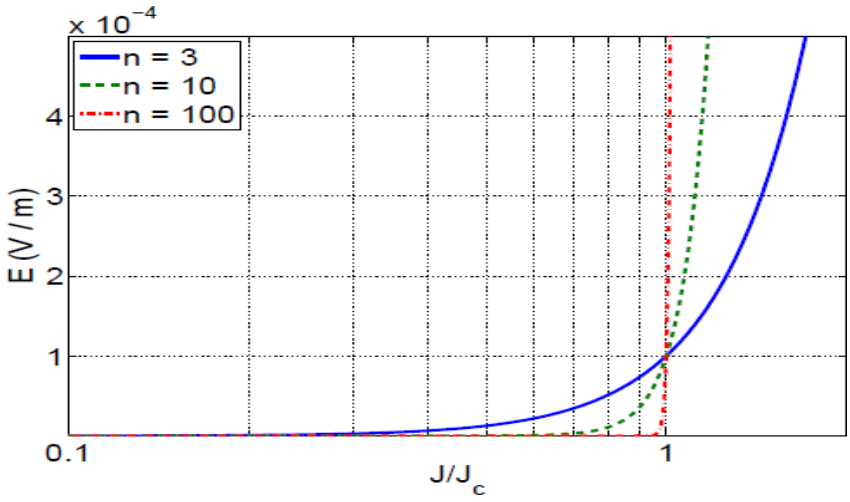

Figure II.2: E (***J***) Characteristic of a Superconductor.**[38]**

II.4. Behavioral Models:

II.4.1. Critical State Model or Bean Model:

The critical state model posits that, at a specified temperature, the current density in a superconductor is either zero or equivalent to the critical current density Jc, making it the predominant model.

$$J=J_c(|B|)\frac{E}{|E|} \qquad \text{(II.3)}$$

$$\overrightarrow{B}=\mu_0 \overrightarrow{H}$$

From a more rigorous mathematical perspective, these formulations are represented by Maxwell's equations:

$$\overrightarrow{rot}\,\overrightarrow{B}=\pm\mu_0\overrightarrow{Jc} \quad \text{ou} \quad \overrightarrow{rot}\,\overrightarrow{B}=\overrightarrow{0} \qquad \text{(II.4)}$$

According to Bean (1962), this model further assumes that the critical current density is invariant and independent of the magnetic induction B. **[39]**

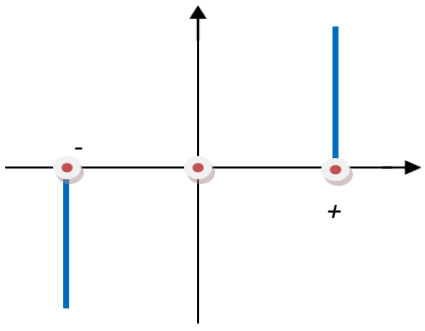

Figure II.3: Characteristic E(J) based on the Bean Model. **[39]**

There are numerous models for calculating current and field distributions while evaluating AC losses in superconductors under various conditions. The most recognized among them is undoubtedly the critical state model, also known as the Bean model.

II.4.2. Power Law Model:

This model effectively encapsulates the behavior of high-critical-temperature superconductors (HTC) near Jc

The mathematical formulation of this model is expressed as follows:

$B(H)=\mu 0H$

The parameters influencing this law include the critical current density Jc and the exponent "n" Through the application of this model, it becomes possible to modify the E(J) curves to simulate a normal conductor for n=1 (linear behavior law) up to obtaining a sharp curve, similar to that observed in the critical state model for n>100

II.4.3. Kim Model:

The Bean model and the power law assume that superconducting materials exhibit isotropic and isothermal characteristics. However, these models do not account for the potential thermal elevation of the conductor resulting from energy losses, which can subsequently lead to a reduction in the critical current. Within the framework of the Bean model, it is assumed that the critical current density remains invariant, regardless of the external magnetic field. In practice, however, this current density is significantly influenced by its orientation relative to the induced magnetic field, B.

An expression defining Jc(B) for the isotropic scenario was introduced by Kim:

$$JC(|B|)=\frac{jc0B0}{|B|+B0} \qquad \text{(II.5)}$$

This is the most widely used model for modelling the critical current density dependence with magnetic induction. **[40]**.

II.4.4. The exponential model:

Another model used in numerical advances is the later dependency model Jc (B).**[6]**

$$J_c(|B|) = J_{c0} \exp\left(-\frac{|B|}{B_0}\right)$$

The Kim and exponential models are the basis of digital advances. In addition, the model proposed by Kim is the predominant choice to represent Jc (B).

II.4.5. Flux Flow Model and Creep Flux:

Two operating modes can be defined for the superconductor, depending on the critical current density Jc:

If $|J| \leq Jc$, the vortex network is immobilized, the vortex network remains anchored; nevertheless, the vortices move from one anchor site to another e" due to thermal fluctuations. This dissipative event is called the "creep" flux regime.

$$E = 2\rho_c J_c \sin h\left(\frac{U0J}{K\theta Jc}\right)\exp\left(-\frac{U0}{K\theta}\right) \quad \textbf{(II.6)}$$

K: Constant of Boltzmann.

θ: Temperature.

ρ_c: Flux Creep Resistivity.

U_0: Potential for depth.

If | J | >Jc, the eddy network becomes mobile, which causes energy losses that induce an electrical resistance in the superconducting material. This event is called the flux flow regime.

$$E = \pm\left(E_c + \rho_f . J_c\left(\frac{|J|}{Jc} - 1\right)\right)\rho_f \quad \textbf{(II.7)}$$

ρf: Flux flow Resistivity

The critical current density can thus be characterized as the threshold separating the creep regime from the flux regime. Given the ambiguity surrounding this threshold, the critical current density is frequently determined using an electric critical field, Ec.**[37]**

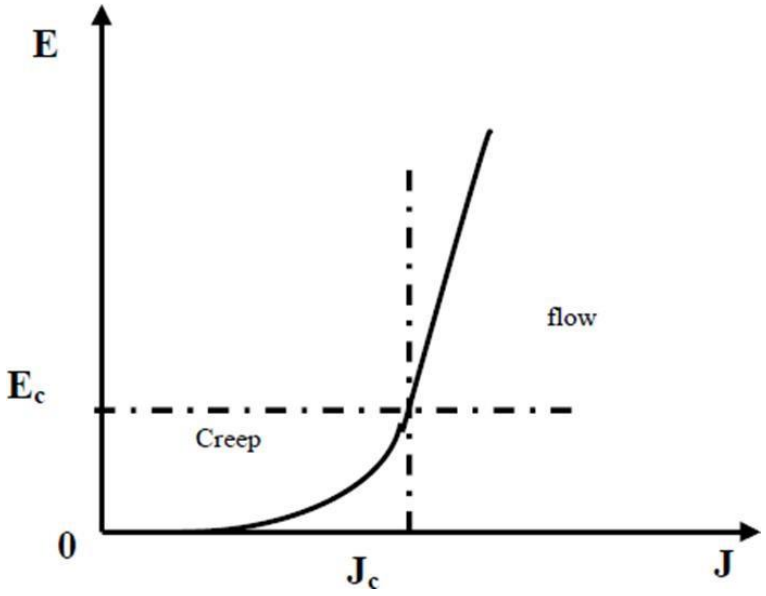

Figure II.4: Flux Flow and Creep Model **[37]**

II. 5. Formulation of Electromagnetic Equations:

The models developed by J.C. Maxwell generally elucidate all electromagnetic phenomena; however, depending on the specific devices studied, some phenomena may become negligible **[41].** Therefore, the equations can be decoupled, giving simplified models. Among these models, we identify: electrostatic, electrokinetic, magnetostatic, and magnetodynamic models..

II.5.1:Electrostatic model [40]:

In this context, the distribution of electrical charges remains independent of time (steady state: DC scenario), so that the generated magnetic field does not fluctuate over time.

$$\frac{\partial \vec{B}}{\partial t} = \vec{0} \quad \text{(II.8)}$$

The equations in this model are simplified as follows:

$$\text{div}\vec{D}=\rho \quad \text{(II.9)}$$

$$\overrightarrow{rot}\vec{E}= \vec{0} \quad \text{(II.10)}$$

$$\vec{D}=\varepsilon \vec{E} \quad \text{(II.11)}$$

We have:

$$\vec{E} = -\overrightarrow{grad}\text{V} \quad \text{(II.12)}$$

The model then comes back to the equation

$$\text{div}(\varepsilon \overrightarrow{grad}\text{V})+\rho=0 \quad \text{(II.13)}$$

II. 5.2 Magnetostatic model:

In this context, the term $\frac{\partial \vec{B}}{\partial t}$ is zero. This is because the magnetic field comes from sources independent of time. Two models exist **[42]:**

II.5.2.1 The Magnetostatic Scalar Model: [40]

In this configuration, the electric currents are zero, resulting in fields that do not vary over time; thus:

$$\overrightarrow{rot}\vec{H}= \vec{0} \quad \text{(II.14)}$$

$$div\vec{B}= 0 \quad \text{(II.15)}$$

$$\vec{B} = \mu\vec{H} \quad \text{(II.16)}$$

$\vec{H}$ Derive from a magnetic scalar potential Φ, hence the nomination of the Scalar magneto static model, such as: $\vec{H}$= - g$\vec{r}$ad Φ

The model then comes back to the equation:

$$\text{Div}(\mu \overrightarrow{grad}\Phi) = 0 \quad \text{(II.17)}$$

II.5.2.2 Vector magneto static model:

In this model, the electric currents are not zero. It comes while that:

$$\overrightarrow{rot}\vec{H}=\vec{J} \quad \text{(II.18)}$$

$$\text{div}\vec{B}=0 \quad \text{(II.19)}$$

$$\vec{B} = \mu\vec{H} \quad \text{(II.20)}$$

The div relation $\vec{B}$=0 allows you to define a vector function, $\vec{A}$Magnetic vector potential, such as:

$$\vec{B}=\overrightarrow{rot}\vec{A} \quad \text{(II.21)}$$

Hence, the equation system:

$$\overrightarrow{rot}(\nu\overrightarrow{rot}\vec{A})=\vec{j} \quad \text{(II.22)}$$

II.5.3 Magneto dynamic model: [40]

This model applies to electromagnetic devices in which the source of current or voltage varies over time. In other words, the term for the temporal variation of the magnetic induction vector is non-zero, which results in the coupling of electric and magnetic fields due to the presence of eddy currents. This model is commonly used in the examination of electrical machines, induction heaters, etc. Equations formulated by J.C. Maxwell can be used to derive equations that describe the spatio-temporal evolution of electromagnetic phenomena. Many formulations exist in the field of electromagnetism. From these formulations, we select the electric field formulation $\vec{E}$ **[40]**

In terms of equations, we have:

$$\overrightarrow{rot}\vec{E} = -\frac{\partial\vec{B}}{\partial t} \quad \text{(II.23)}$$

$$\overrightarrow{rot}\vec{H} = \vec{j} \quad \text{(II.24)}$$

To these equations, we add the laws characteristic of the

Environment:

$$\vec{B} = \mu\vec{H} \quad \text{(II.25)}$$

$$\vec{D} = \varepsilon\vec{E} \quad \text{(II.26)}$$

By taking the rotational:

$$\overrightarrow{rot}\overrightarrow{rot}\vec{E} = -\overrightarrow{rot}\frac{\partial\vec{B}}{\partial t} \quad \text{(II.27)}$$

Replacing equation (II.25) in (II.27), we get:

$$\overrightarrow{rot}\,\overrightarrow{rot}\,\vec{E} = -\overrightarrow{rot}\frac{\partial\mu\vec{H}}{\partial t} \quad \text{(II.28)}$$

We consider μ constant over time, from which the preceding equation becomes:

$$\overrightarrow{rot}\overrightarrow{rot}\vec{E} = -\mu\frac{\partial\overrightarrow{rot}\,\vec{H}}{\partial\,t} \quad \text{(II.29)}$$

Finally, we get:

$$\overrightarrow{rot}\overrightarrow{rot}\vec{E} = -\mu\frac{\partial\vec{j}}{\partial t} \quad \text{(II.30)}$$

With:

div$\vec{E}$ = 0(no charge)

We have:

$$\Delta\vec{E} = \mu\frac{\partial\vec{j}}{\partial t} \quad \text{(II.31)}$$

Where:

$$(\text{div}\overrightarrow{grad})\,\vec{E} = \mu\frac{\partial\vec{j}}{\partial t} \quad \text{(II.32)}$$

II.6.Conclusion:

In this section, we have explored various formulations of the electromagnetic problem and the mathematical frameworks necessary for modeling high-temperature superconducting materials (SH Tc). Our primary emphasis was on the magnetostatic model within a superconducting medium, employing the magnetic vector potential approach. The numerical modeling of electromagnetic phenomena in superconductors presents several challenges. We developed a numerical methodology for simulating superconducting materials using the PDETOOL/MATLAB software, which addresses the solution of Maxwell's equations, known for their significant non-linearity. The next chapter will delve into the study of superconducting coils, their manufacturing processes, their effects on new configurations of superconducting transformers, and the incorporation of superconducting materials into these transformers.

CHAPTER III

Application and Results of simulation

III.1 Introduction :

The main objective of this chapter is to conduct an in-depth comparison between autotransformers using superconducting materials and those based on conventional materials. To achieve this, the finite element method (FEM) will be applied using PDETOOL in MATLAB. This tool allows for a detailed analysis of the various physical and electromagnetic aspects of the autotransformer, highlighting the significant differences between the two types of systems.

The use of MATLAB ensures highly accurate simulation results, enabling clear differentiation between a superconducting autotransformer and a conventional one. The study will focus on key performance indicators such as magnetic field distribution, current density, energy losses (particularly Joule losses), and overall efficiency and thermal behavior.

This comparative analysis will help deepen the understanding of both the advantages and limitations of each type of autotransformer. In particular, the unique properties of superconducting materials, such as their ability to eliminate resistive losses, will be closely examined and contrasted with the performance of traditional conducting materials.

Finally, detailed observations will be recorded to document all simulation outcomes. These findings will form the basis for a comprehensive evaluation of the performance of superconducting autotransformers compared to their conventional counterparts. The aim is to provide valuable insights for optimizing autotransformer designs and to support the ongoing development of superconducting technologies in the field of power conversion and energy distribution.

III.2 Definition of an Autotransformer :

An autotransformer is a type of electrical transformer that operates based on the principle of electromagnetic induction, but unlike conventional transformers, it consists of a single continuous winding that acts simultaneously as both the primary and secondary winding. The winding features one or more tapped points that allow a portion of the winding to serve as a voltage transformation. This design enables the autotransformer to step up or step down alternating current (AC) voltages while maintaining the same frequency and waveform, with the added benefit of increased efficiency, reduced size, and lower cost compared to traditional two-winding transformers. However, because the primary and secondary circuits share a common winding, electrical isolation is not provided, which limits its application in systems where galvanic isolation is required. Autotransformers are widely used in applications such as motor starting, voltage

regulation in power systems, and audio systems, especially when the voltage ratio is close to unity [43-44]

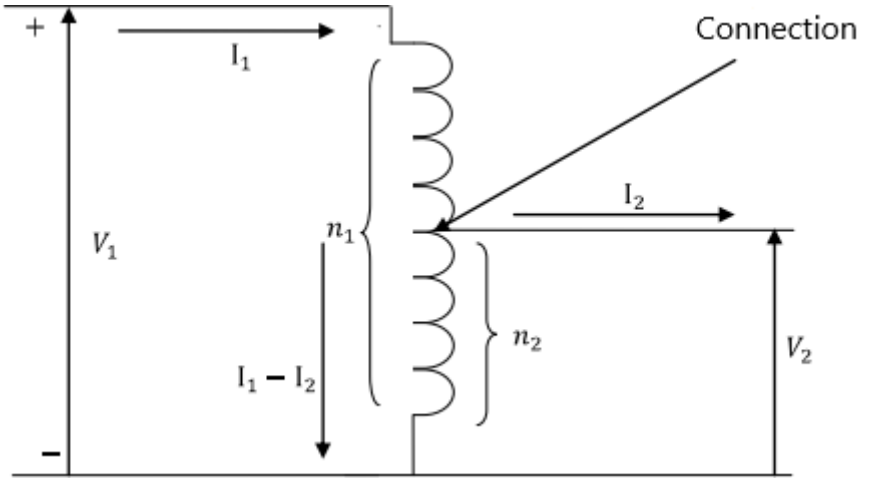

Figure.III.1: The constitution of an autotransformer.

III.3 Historical Background of the Autotransformer:

The autotransformer emerged as an important variant of the conventional transformer in the early 20th century, following the widespread adoption of standard transformers in electric power systems. While the fundamental principle of electromagnetic induction remains the same, the autotransformer distinguishes itself through a single continuous winding with a variable tap, rather than the separate primary and secondary windings found in traditional designs. Early studies and implementations of autotransformers were motivated by the need for compact, cost-effective, and energy-efficient solutions in systems where voltage ratios were relatively close to unity. Their reduced size, lower copper requirements, and higher efficiency made them ideal for specific applications such as voltage regulation, motor starting, and railway electrification. [43]

Although autotransformers were initially limited in application due to the lack of electrical isolation between the input and output, their advantages in certain configurations have led to widespread use, particularly in industrial environments and power transmission systems where space and cost are significant considerations. The development of tap-changing mechanisms and improvements in insulation technologies have further enhanced the functionality of autotransformers, enabling their integration into modern high-voltage substations and even HVDC systems. Today, autotransformers continue to play a critical role in optimizing voltage profiles and improving system stability in complex power networks. [45]

III.4 The operating principle of the Autotransformer :

The operating principle of an autotransformer is based on the phenomenon of electromagnetic induction, similar to that of a conventional transformer. However, unlike conventional transformers, an autotransformer uses a single continuous winding that serves both the primary and secondary circuits, with a portion of the winding common to both. This configuration allows for a more compact and cost-effective design. When an alternating current (AC) flows through the input terminals, it generates a time-varying magnetic field within the core, which induces a voltage across the winding according to Faraday's Law of induction. The voltage transformation depends on the tap point chosen along the winding, which determines the number of turns associated with the primary and secondary sides. Because part of the winding is shared, autotransformers exhibit improved efficiency and lower losses compared to traditional transformers, especially in applications where the voltage difference between input and output is relatively small. Autotransformers are widely employed in voltage regulation, motor starting, and power distribution systems, where compact size, efficiency, and cost are key considerations. [44] [46]

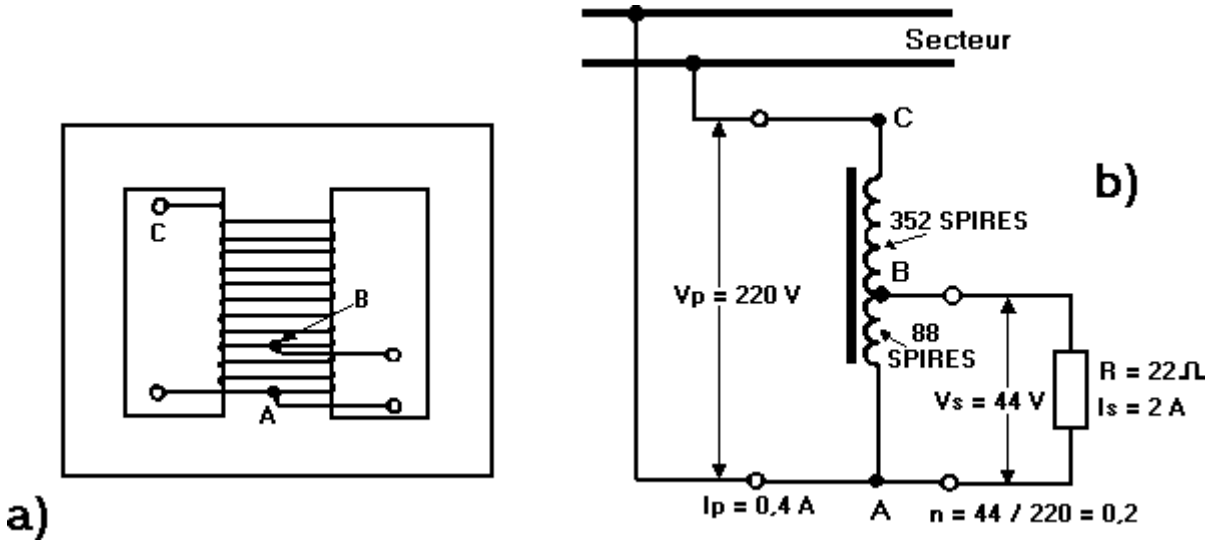

Figure.III.2: Step-Down Autotransformer

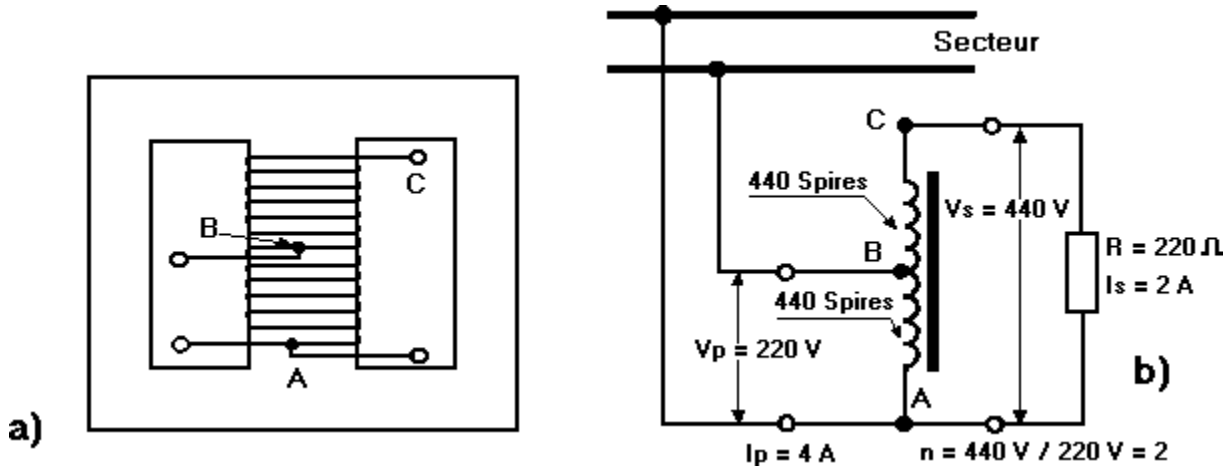

Figure.III.3: Elevator Autotransformer

III.5 The constitution of an autotransformer :

The constitution of an autotransformer is based on a single continuous winding wound on a laminated magnetic core, typically made of silicon steel sheets to reduce eddy current losses. Unlike conventional transformers, which have two separate windings (primary and secondary), the autotransformer uses a common winding that acts simultaneously as both the primary and secondary. Specific points along the winding are tapped to provide the desired output voltage, and the portion of the winding shared between input and output allows for direct electrical connection. The remaining portion, connected either above or below the tap point, contributes to the voltage transformation by electromagnetic induction. This structural design significantly reduces the amount of copper wire and core material required, making autotransformers lighter, smaller, and more efficient than their double-winding counterparts, particularly in applications with a small voltage difference. However, due to the absence of galvanic isolation between input and output circuits, autotransformers are not suitable where safety isolation is required. They are commonly used for voltage regulation, motor starting, and voltage conversion in power distribution systems, where efficiency and material savings are critical. [47]

III.6 Characteristics of an Autotransformer:

An autotransformer is an electrical device designed to modify the voltage of an alternating current using a single continuous winding with one or more tapping points, rather than two

separate windings as in conventional transformers. This construction leads to several unique features that distinguish it from traditional transformers. [43]

III.6.1 Rated Power (kVA):

This is the maximum power the autotransformer can deliver under standard operating conditions. It is expressed in kilovolt-amperes (kVA). Due to shared windings, autotransformers often offer higher efficiency and greater power density compared to two-winding transformers.

III.6.2 Frequency (Hz):

The operating frequency is typically 50 or 60 Hz, aligning with standard AC electrical systems.

III.6.3 Input and Output Voltages:

The input voltage is applied across the full winding, while the output is taken from a tap along the same winding. Both are expressed in volts (V).

III.6.4 Input and Output Currents:

The current in each section of the winding is dependent on the load and the tap configuration, and is measured in amperes (A).

III.6.5 Transformation Ratio:

The ratio of input voltage to output voltage, expressed as “n:1”, depends on the position of the tapping point on the winding. This ratio determines whether the autotransformer steps up or down.

III.6.6 Common Winding:

Unlike conventional transformers, autotransformers use a portion of the same winding for both primary and secondary circuits. This results in reduced copper losses, lower cost, and compact size.

III.6.7 Cooling Method:

Depending on the power rating and installation, autotransformers may be cooled by air (dry type) or oil (liquid-immersed). Cooling influences both efficiency and operational lifespan.

III.6.8 Standards:

Autotransformers must comply with safety and performance standards such as IEC 60076 and IEEE C57.96, which define the technical and quality requirements for commercial use.

III.6.9 Applications:

Common applications include motor starting, voltage regulation, HVAC systems, railway traction, and interconnection of networks with similar voltage levels.

III.6.10 Technologies:

Autotransformers can be single-phase or three-phase, and are manufactured using either dry-type or oil-immersed construction depending on environmental and performance needs.

III.7 The Superconducting AutoTransformer :

A superconducting autotransformer is an advanced form of autotransformer that employs high-temperature superconducting (HTS) materials to reduce power losses and improve efficiency. Unlike conventional autotransformers, which rely on copper or aluminum conductors and operate at ambient temperatures, superconducting autotransformers function at cryogenic temperatures using liquid nitrogen or helium cooling systems to maintain superconductivity in their windings [48], [49]. This design allows for extremely low electrical resistance, resulting in minimal I^2R losses and improved power density. Due to their shared winding structure, autotransformers already offer material savings and compactness; integrating superconductors further enhances these benefits by enabling smaller, lighter, and more efficient systems.

Such devices are especially suitable for high-power applications, such as electrical grids, railway systems, and industrial motors, where reducing transmission losses and optimizing space are key priorities [50]. However, the widespread adoption of superconducting autotransformers is still limited by technical and economic challenges, such as the cost of superconducting materials, the complexity of cryogenic systems, and the need for robust thermal insulation. Additionally, modeling such systems involves dealing with nonlinear magnetic and thermal properties, making simulation and design highly dependent on finite element analysis (FEA) and advanced magneto-thermal coupling models [51].

In this context, our study applies magnetostatic approximations based on Maxwell's equations to evaluate the performance of superconducting autotransformer configurations. Using the finite

element method (FEM) via tools such as MATLAB PDE Toolbox, we assess magnetic field distribution, thermal dissipation, and the overall magnetothermal behavior of the system. This comparative analysis between superconducting and conventional autotransformer designs aims to highlight the performance gains and pinpoint practical limitations, thereby guiding future improvements in the development of next-generation energy-efficient transformers.

III.8 Presentation of the proposed model:

The model proposed in this work is based on a superconducting autotransformer structure composed of a ferromagnetic core with two possible configurations:

First configuration: A traditional autotransformer with a single continuous copper winding and tap connections to provide different voltage levels.

Second configuration: A hybrid autotransformer using a superconducting material in part of the winding,

This design aims to take advantage of superconducting properties within the autotransformer concept, where a single winding serves both voltage input and output, depending on the tap points.

III.8.1 Parameters of the studied geometry:

The basic parameters for the Autotransformer design are displayed in Table III.1.

parameters	values
Apparent power (S)	10 kVA
Power supply frequency (f)	60 Hz
Voltage (Vpri)	600 V
current (Ipri)	16.6667 A
ambient temperature (T)	295 K
Maximum temperature (T)	348 K
Coefficient of convection h	10 W/ (m2.K)
conventional coil	copper
superconducting coil	YBCO

Table III.1: Parameters of the geometry studied

III.8.2 Description géométrique:

The geometrical description is the first stage in the process of implementing the mathematical model. Before proceeding, the different parts of the autotransformer and their physical parameters are defined.

This section provides a general overview of the geometry and finite element meshing. The aim is to help the reader understand the structure of the autotransformer, including the winding layout, magnetic core, and physical boundaries as illustrated in Figures III.5, III.6, and III.7.

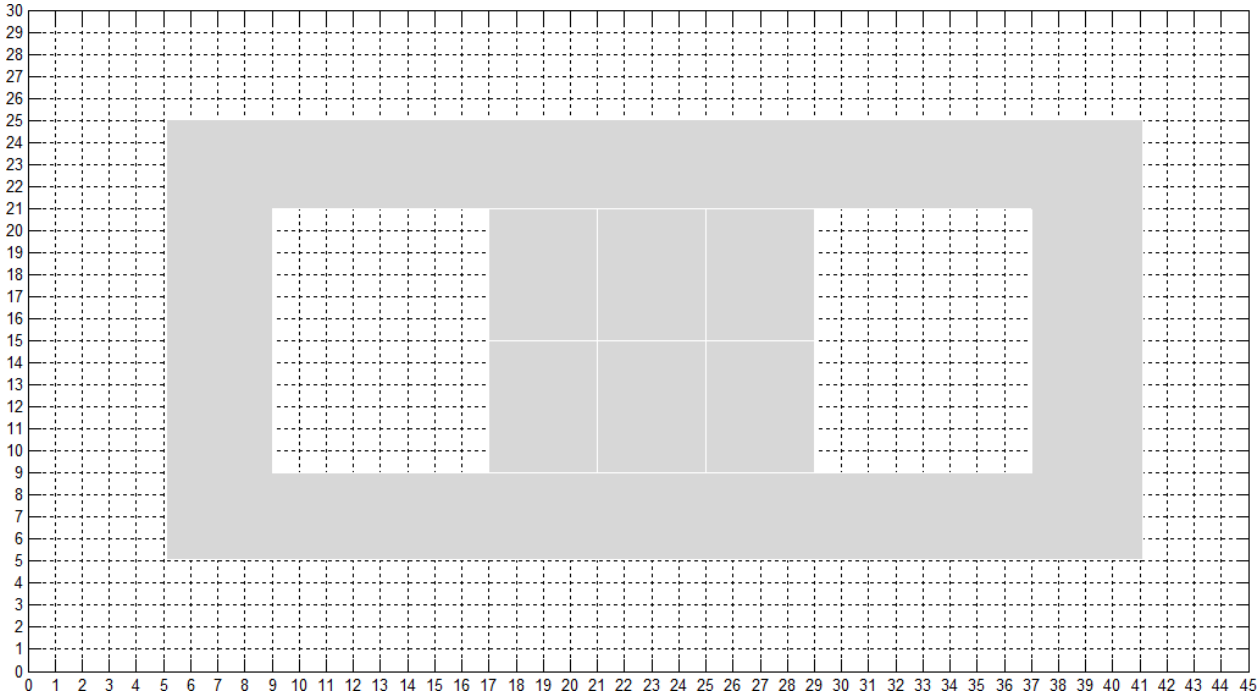

Figure.III.4: Geometry creation.

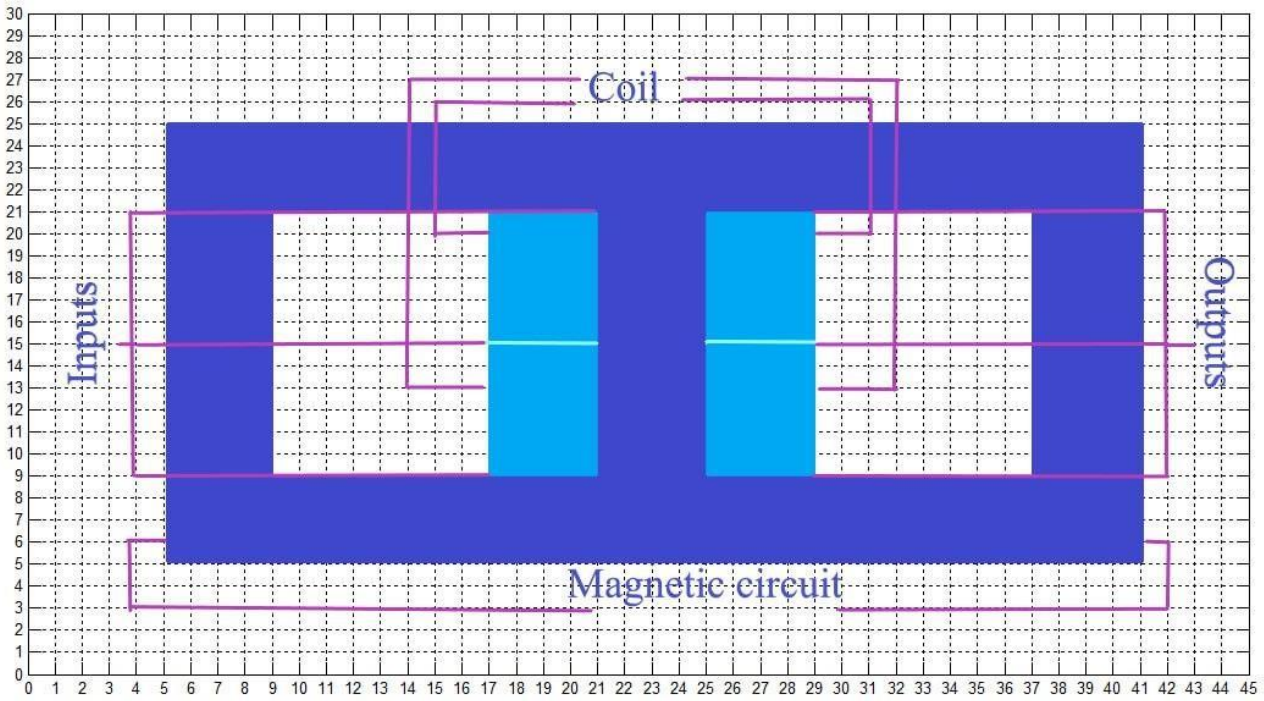

Figure.III.5: Positions of the coil

As shown in Figure III.5, the single coil is located in the middle of the ferromagnetic core, with voltage taps positioned at specific locations according to the transformation ratio.

A finite element mesh is applied to the entire structure, allowing for accurate simulations of electromagnetic and thermal behavior.

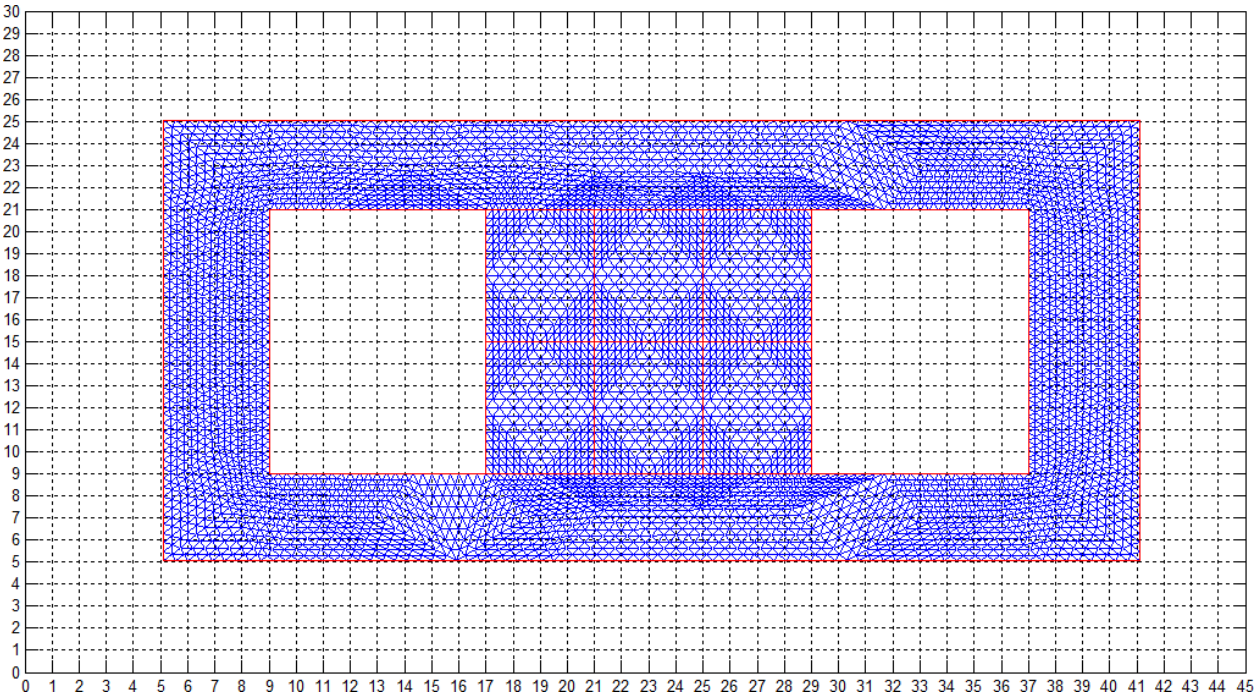

Figure.III.6: Mesh structure of the core generated by the FEM.

III.9 Different simulation results:

The following simulations present distributions of magnetic flux, magnetic field, temperature, and current density for the studied prototypes. These results are obtained using equations that link electromagnetic quantities within the ferromagnetic and superconducting materials used in the model.

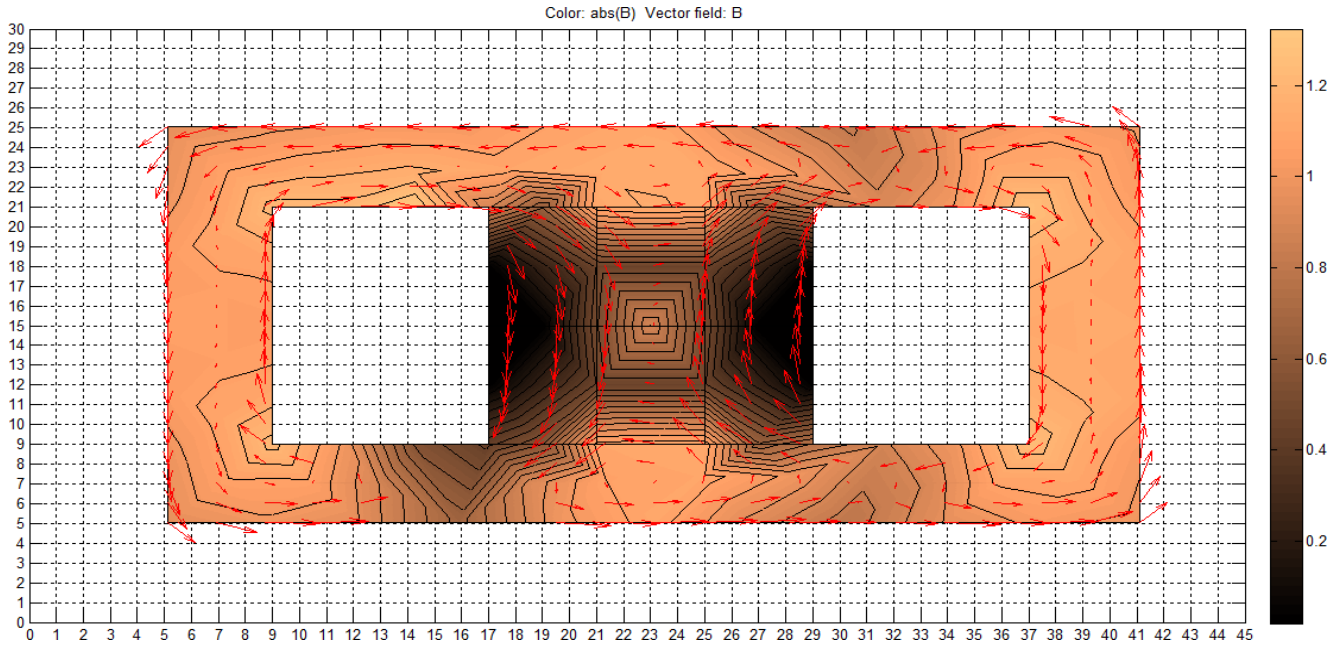

(a) Autotransformer Classic.

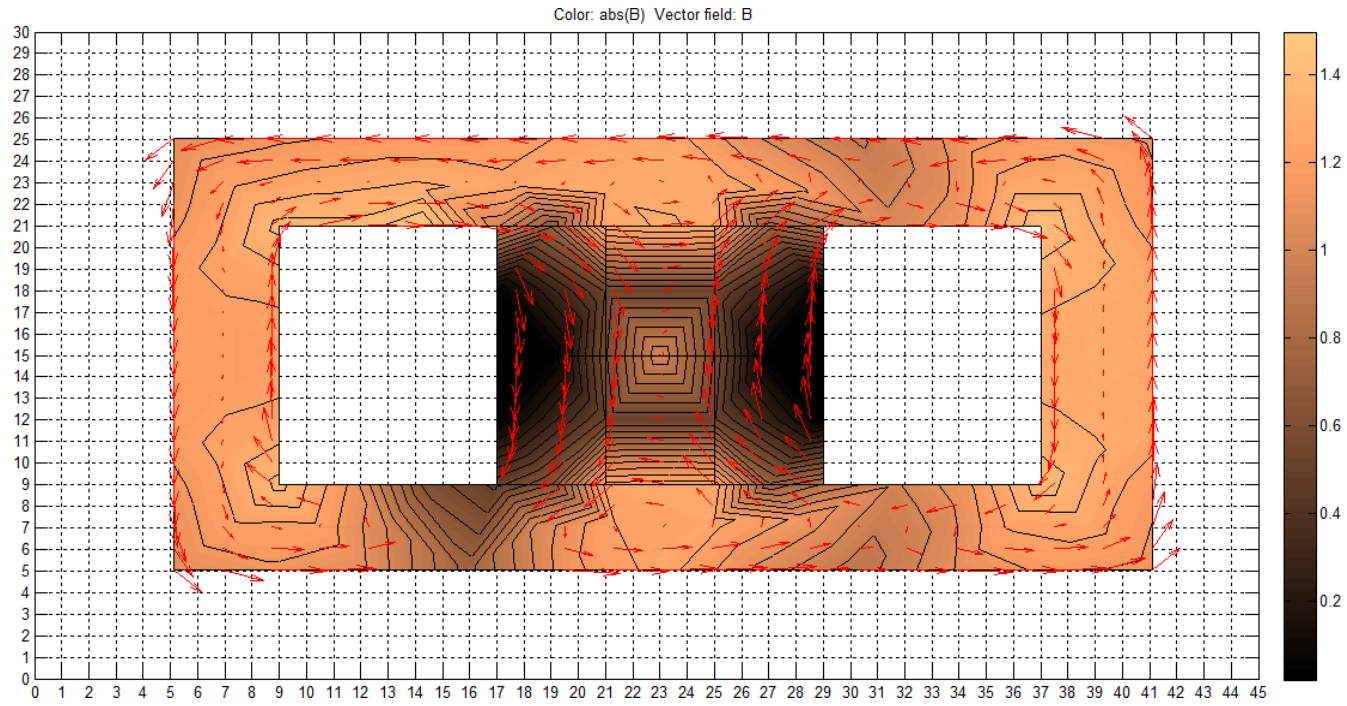

(b) Superconducting autotransformer.

Figure.III.7: Appearance of the magnetic flux

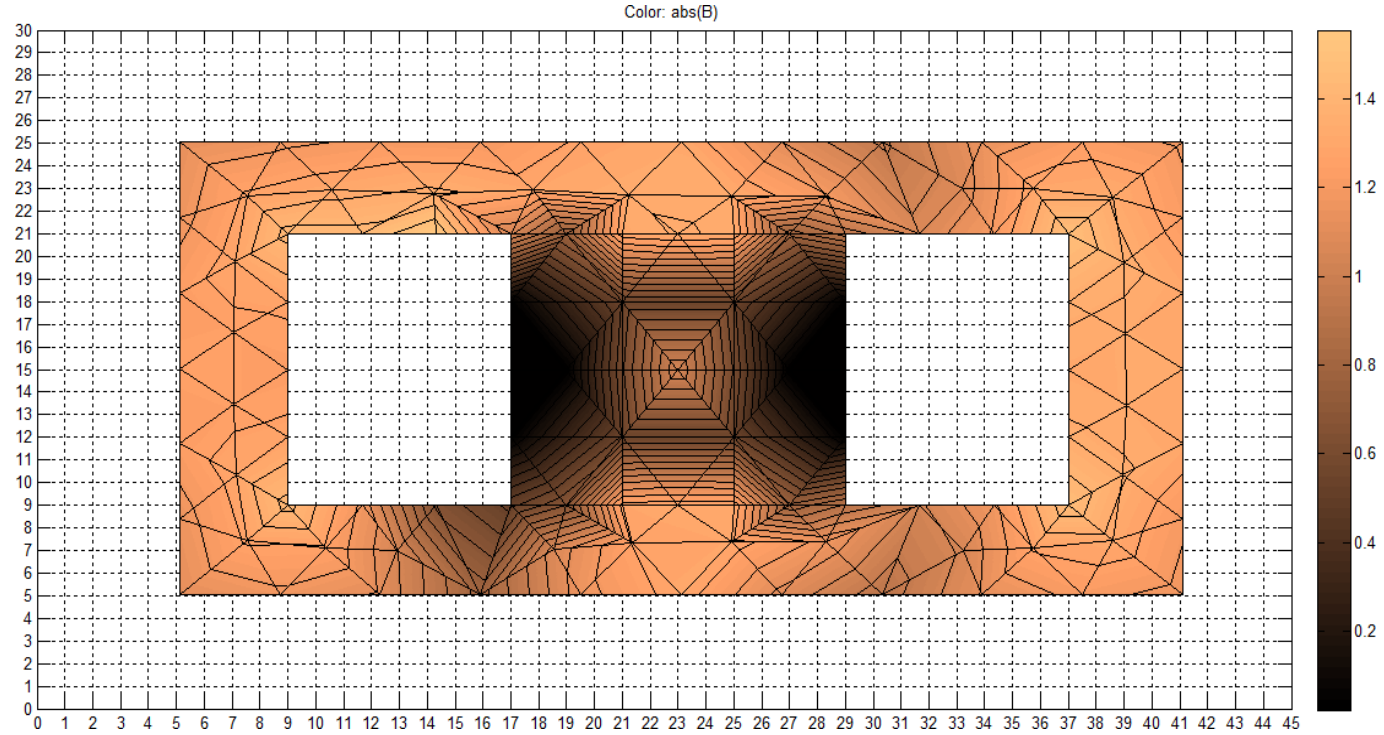

(a) Autotransformer Classic.

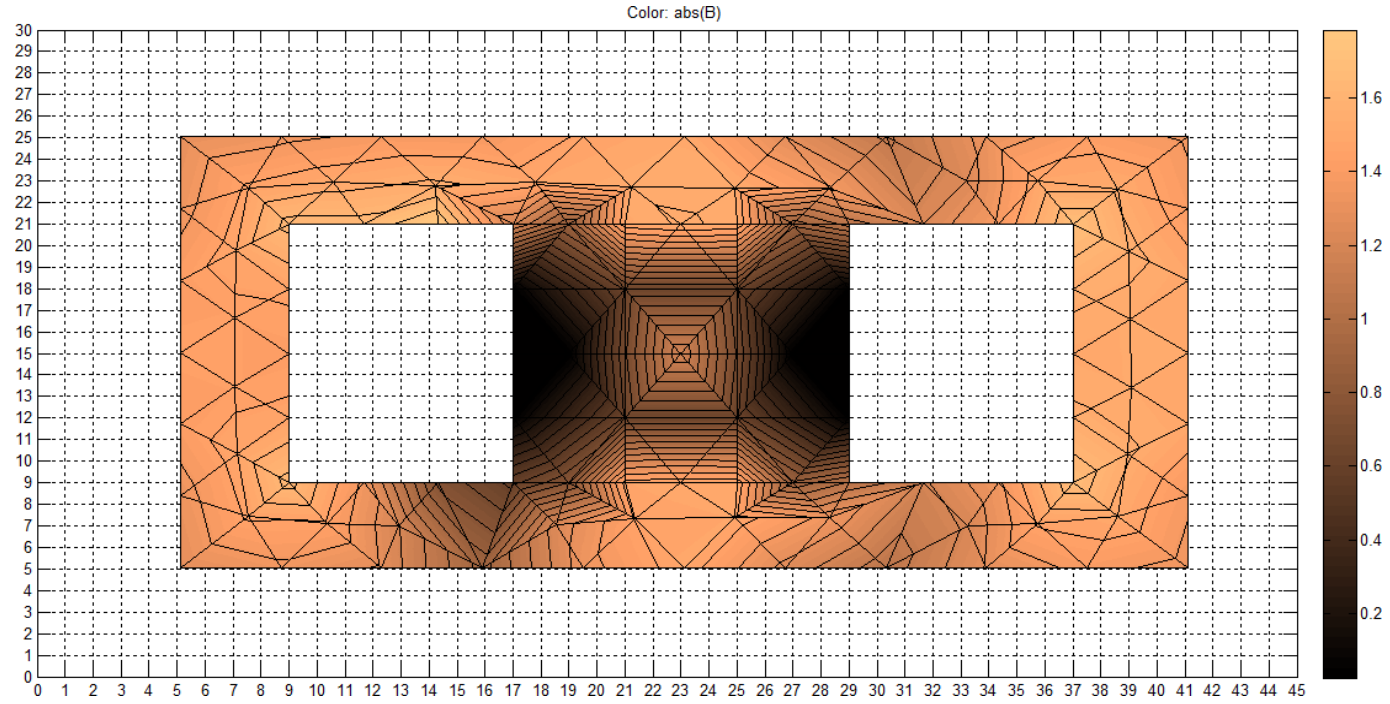

(b) Superconducting autotransformer.

Figure.III.8: The distribution of magnetic flux density

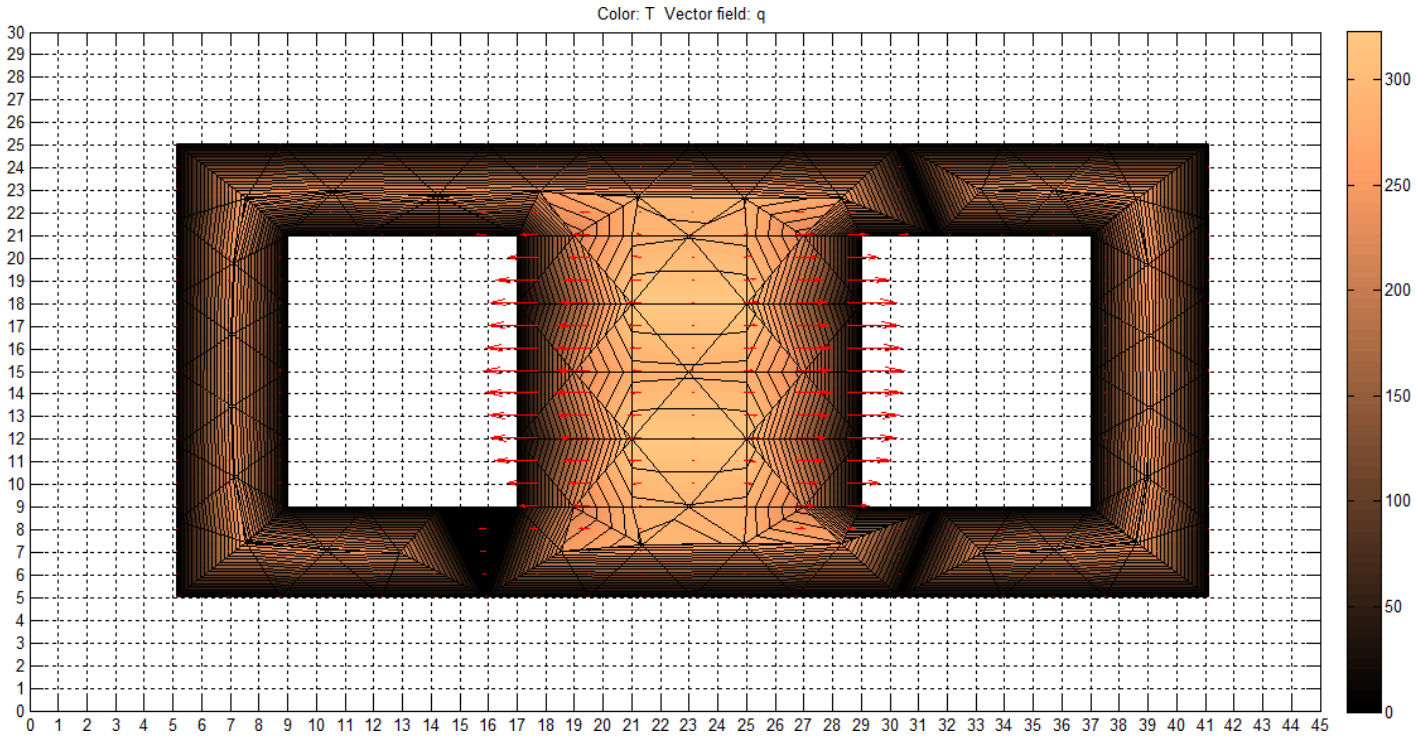

(a) Autotransformer Classic.

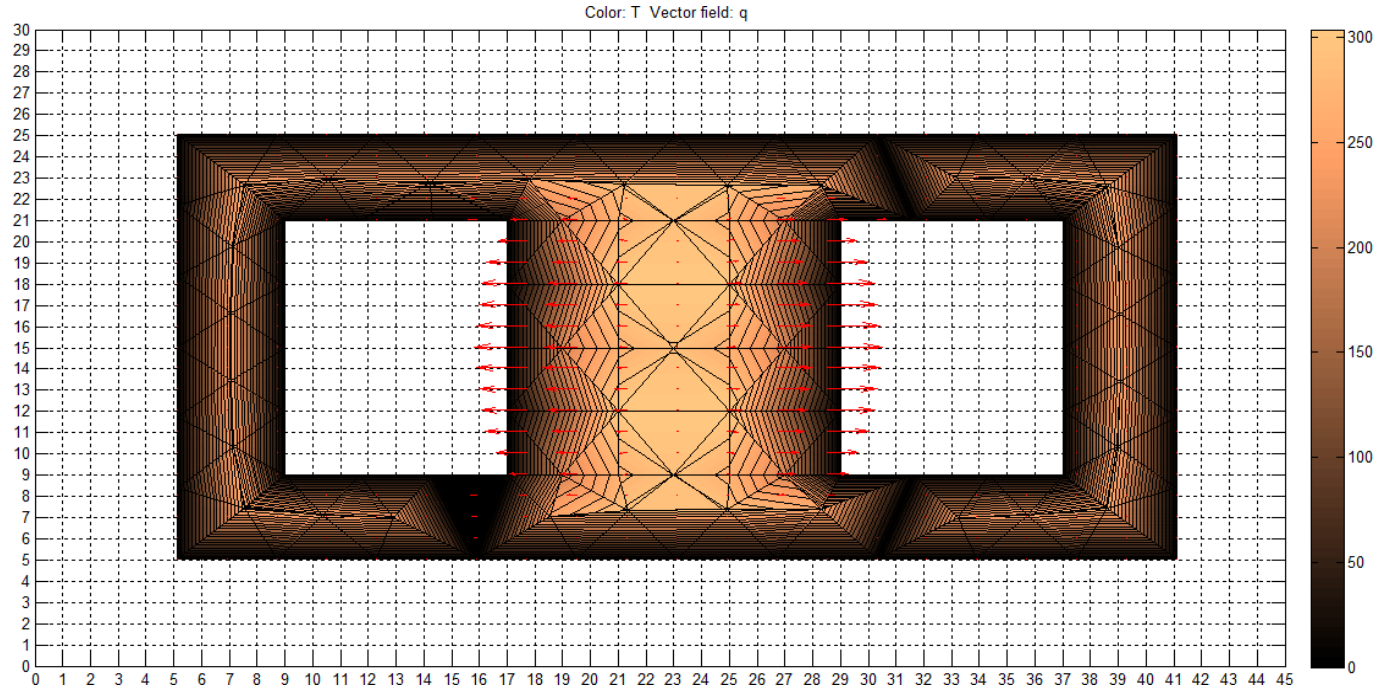

(b) Superconducting Autotransformer.

Figure.III.9: Temperature profile

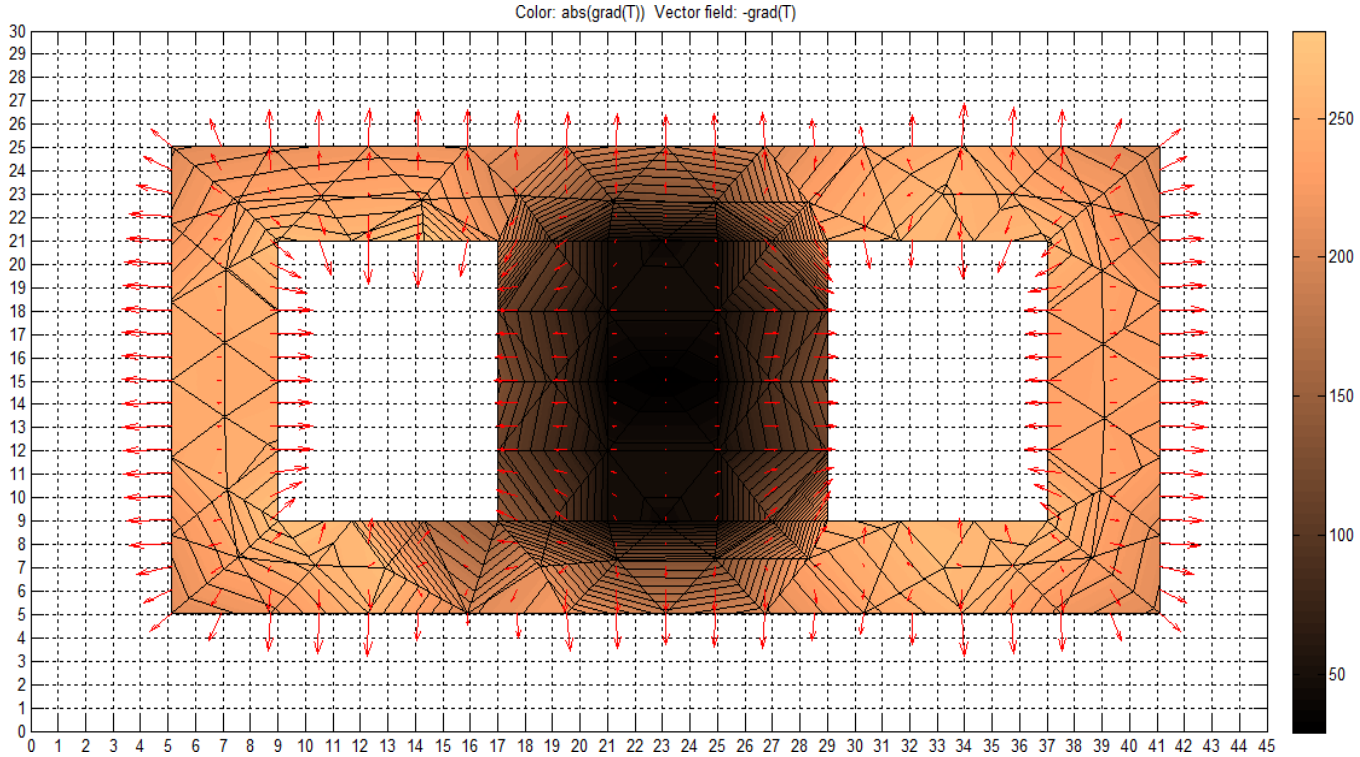

a) Autotransformer Classic.

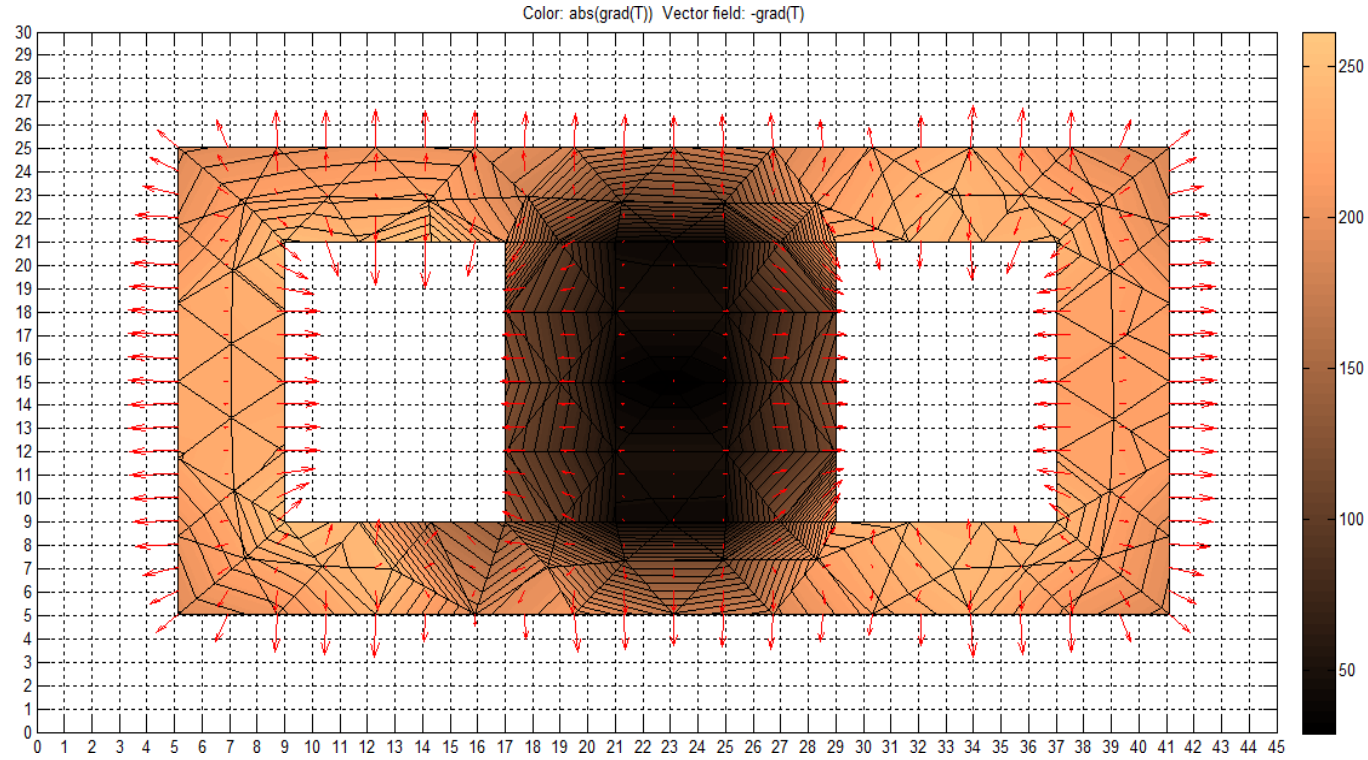

(b) Superconducting Autotransformer.

Figure.III.10: Temperature gradient profile

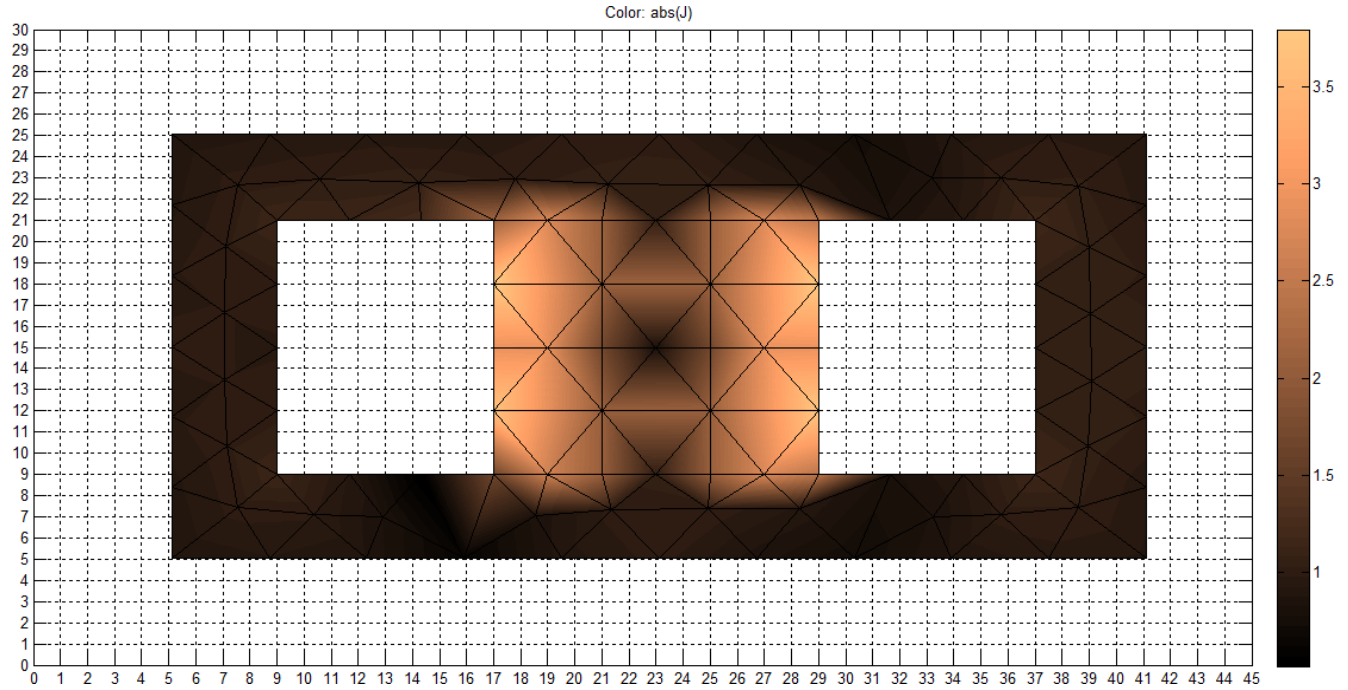

(a) Autotransformer Classic.

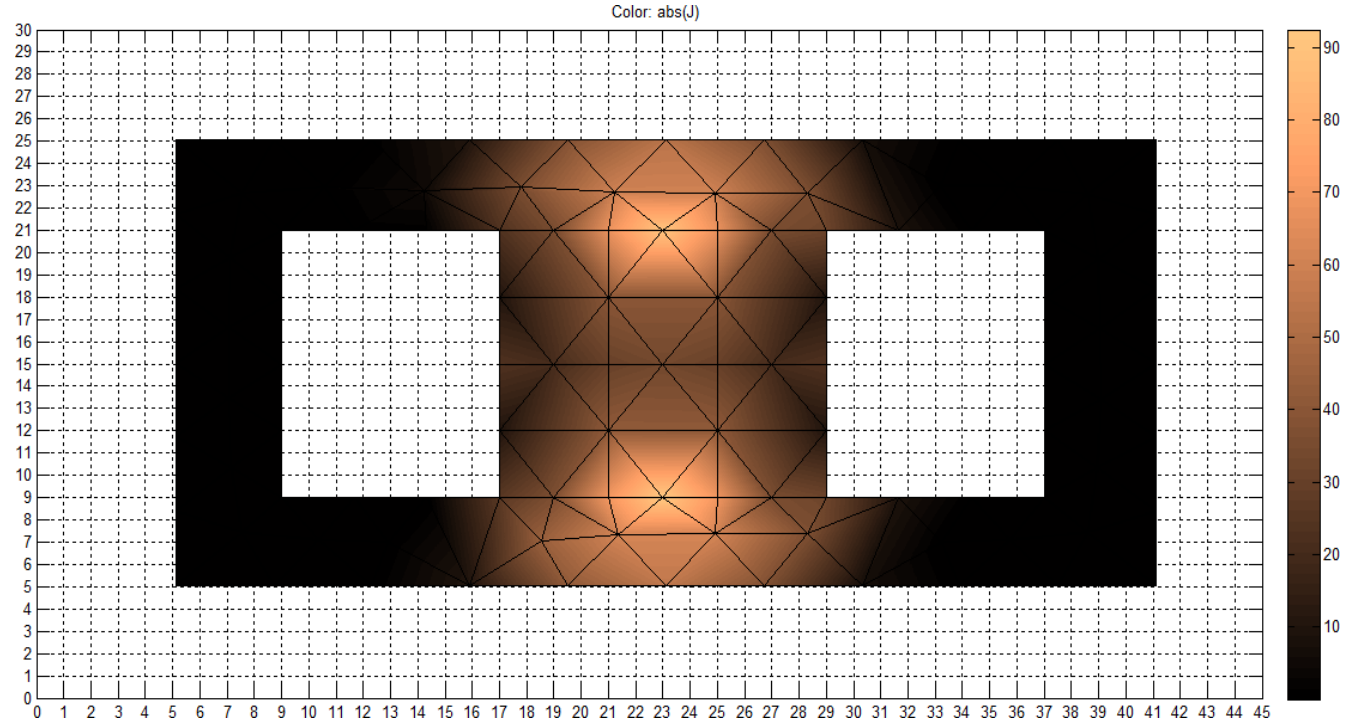

(b) Superconducting Autotransformer.

Figure.III.11: Current density profile

III.10 Interpretation of Results:

The figures above show different results obtained

Appearance of the magnetic flux (Figure III.7):

The magnetic flux is primarily concentrated in the ferromagnetic core, which is consistent with expected behavior. The flux paths are continuous and well-guided through the core, validating the efficiency of magnetic coupling.

In the superconducting configuration, the magnetic flux appears more confined and well-channeled, highlighting improved magnetic performance due to the perfect diamagnetism of superconducting materials. This translates into reduced losses and better field control.

The distribution of magnetic flux density (Figure III.8):

In a conventional autotransformer, magnetic induction is fairly distributed across the core, though localized saturation may occur. With a maximum set to 1.6 T, the effective induction in different parts of the core is about 0.8 T.

In contrast, the superconducting autotransformer shows a more uniform and higher magnetic induction, up to 1.8 T, with reduced losses and stronger magnetic field control. This illustrates the benefits of integrating superconducting material into the winding.

Temperature profile (Figure III.9):

The conventional autotransformer shows significant thermal gradients, with central zones reaching up to 330 K, likely due to Joule heating from resistive losses.

The superconducting autotransformer shows a more uniform temperature profile, around 305 K, thanks to the absence of resistive heating. This results in better thermal management and improved lifespan of the device.

Current Density (Figure III.11):

In the copper-based autotransformer, current density is uneven and concentrated near the taps, with values around 1.9 A/mm² and 3.8 A/mm² depending on location.

In the superconducting autotransformer, current density is much higher (up to 92 A/mm² in the YBCO region) and more evenly distributed due to the zero-resistance property of superconductors. This allows the device to carry more current with virtually no energy loss.

III.11 Conclusion:

The comparative study conducted using the finite element method with PDETOOL in MATLAB revealed significant differences between conventional and superconducting autotransformers.

The superconducting autotransformer shows notable advantages in terms of energy efficiency, loss reduction, thermal management, and power density. While the use of superconducting materials entails higher initial costs and technical complexity, the performance gains can justify their integration in high-performance power systems.

Summary of Advantages and Disadvantages:

Superconducting autotransformers offer: Superior electrical efficiency, Lower thermal and magnetic losses, Compact and lightweight design, Uniform temperature and current distribution.

However, challenges such as High initial costs, cooling requirements, Complex fabrication, and control systems must be considered when evaluating their viability.

In conclusion, although superconducting autotransformers face engineering and cost-related challenges, their potential to significantly enhance the performance and reliability of electrical networks makes them a promising technology. Continued research and improvements in superconducting materials and cryogenic systems could enable broader adoption in future sustainable power infrastructure.

General Conclusion

General Conclusion:

This work focuses on the study and modeling of two-dimensional electrical autotransformers that incorporate high-temperature superconducting (HTS) materials. The aim is to explore the structure and performance characteristics of a superconducting autotransformer. To achieve this, the Finite Element Method (FEM) was employed, taking into account the electromagnetic properties of the materials used.

Various results were independently analyzed using specialized simulation tools. Following multiple simulations, a comparative study was conducted focusing on the distribution of current density, magnetic flux density, and temperature within two proposed autotransformer designs. The significant discrepancies observed between the models confirm that superconducting materials offer substantial benefits and can be effectively utilized in autotransformer applications. Specifically, they enable high current densities and contribute to improving the power factor of the electrical system.

The numerical modeling approach was carefully optimized to reduce energy losses in autotransformers entirely based on superconducting materials, thereby simplifying their design and enhancing their overall efficiency.

The methodology of this study can be summarized as follows: Initially, an in-depth analysis of the properties of superconducting materials was performed.

In Chapter 1, it was demonstrated that HTS materials are increasingly used in the electrical industry due to their ability to significantly enhance autotransformer performance, particularly through their lossless electrical conduction and ability to operate at elevated temperatures, which also contributes to improved energy storage capacity.

In Chapter 2, we emphasized the critical importance of mathematical modeling and theoretical analysis of superconducting materials as a prerequisite for their integration into simulation platforms. This foundational step served as the basis for the simulations and analyses carried out in the following chapters.

Finally, in Chapter 3, we succeeded in improving several key parameters that characterize the autotransformer. This was achieved by reducing losses associated with Joule heating, which manifests as thermal dissipation, and by increasing the current density, thereby enhancing the magnetic flux density within the magnetic core.

This study naturally opens the door to several potential extensions, including:

- The implementation of a practical experimental test.
- Further investigation into the integration of autotransformers in external flux systems.
- The use of additional simulation platforms, such as ANSYS or COMSOL Multiphysics, for modeling and validation.

REFERENCES

Bibliographic References:

[1] Lévêque, J., Berger, K., Lubin, T., &Douine, B. (2018). Moteurs et générateurs supraconducteurs. La Revue 3 E. I, 94, 34-35.

[2] Belkhiri, S. (2004). Contribution à l'étude des frontières libres de conduction et des pertes dans les fils supraconducteurs de type II massifs avec la loi de conduction idéale de BEAN (Mémoire de magistère, Batna, Université El Hadj Lakhder. Faculté des sciences de l'ingénieur).

[3] RENAUD MOULIN. "Dimensionements et essais de moteurs supraconducteurs'" Doctoral thesis of the Université Henri Poincaré, Nancy 1, 2010.

[4] Tnourji, A. (2019). les caractéristiques des matériaux supraconducteurs (mémoire de magistère université chermoutauverge).

[5] M. K. Wu, J. R. Ashburn, C. J. Torng, P. H. Hor, R. L. Meng, L. Gao, Z. J. Huang, Y. Q.

[6] Belkhiri, S., Ghemari, Z., Khene, M. L. , Ben Mebarek, F. and Saad, **S.**(2022). Implantation of Coated Superconducting Materials in the Synchronous Machine for Superconducting Energy Storage , Journal of New Materials for Electrochemical Systems, vol. 25, nº. 4, pp. 277-285.

[7] Belkhiri, S., Bouroubi, M., &Harrabi, A.(2020). Improvement of the Transient Stability of a 14-bus Network Using a Superconducting Fault-Current Limiter SFCL. Advanced Electromagnetics, 9(2), 75-83.

[8] Belkhiri, S., Ghemari, Z. (2022). Comparative Study of Solid and Thin-Layers Superconducting Fault Current Limiters SFCL for Electrical Network Transient Stability Improvement ». Journal of Superconductivity and Novel Magnetism. vol. 35, nº 3, pp.679-688.

[9] Wang, Z. S. (2012). The superconducting properties research of iron based-122 by transport and scanning micro-squid measurements, Thèse de doctorat, Université de Grenoble ;Académie des sciences de l'Université de Chine.

[10] Bouchekhou, H. (2019). Étude d'une machine synchrone à base d'éléments supraconducteurs, Thèse de doctorat ,Université Mohamed SeddikBenyahia - Jijel.

[11] Leclerc, J. (2013). Méthodes et outils de caractérisation électrique et magnétique des supraconducteurs, Thèse de doctorat, Université de Lorraine.

[12] P. TIXADOR, "Matériaux Supraconducteurs". Lavoisier, Hermès Sciences Publication, Paris, 2003

[13] L-P LEVY, "Magnétisme et supraconductivité", CNRS Editions, 1997..

[14] Tnourji, A. (2019). Les caractéristiques des matériaux supraconducteurs» Article.

[15] Elbaa, M. (2020). Caractérisation et modélisation des matériaux supraconducteurs à haute température critique, Thèse de doctorat, Université de Lorraine; Université de Laghouat (Algérie).

[16] ABDERREZAKk, A. (2005). Etude des propriétés structurales, électriques et magnétiques de céramiques supraconductrices YBaCuO et BiSrCaCuO, Thèse de doctorat, Université Mentouri Constantine.

[17] BOUMARAF, R. (2014**).** Modélisation par la méthode des volumes finis modifiés 3D d'une machine électrique supraconductrice, Thèse de doctorat, Université Mohamed Khider– Biskra.

[18] Alhasan, R. (2015). Étude et Réalisation d'une Nouvelle Structure d'un Moteur synchrone supraconducteur. Thèse doctorat de l'université de Lorraine.

[19] Mechekkef, Z., Ayadi, A. (2020).Etude de comportement d'un matériau supraconducteur. Mémoire de Master, Université de Jijel.

[20] Source :http://www.neel.cnrs.fr

[21] Tinkham, M. (2004). *Introduction to Superconductivity* (2nd ed.). Dover Publications. Provides an in-depth discussion of the distinctions between Type I and Type II superconductors and their respective technological applications.

[22] Blundell, S. J. (2001). *Magnetism in Condensed Matter*. Oxford University Press. Discusses the magnetic properties of materials, including the behavior of Type II superconductors in external fields.

[23] Bednorz, J. G., & Müller, K. A. (1986). "Possible High Tc Superconductivity in the Ba-La-Cu-O System." *ZeitschriftfürPhysik B*.

[24] Renaud M. (2010). Dimensionnements et essais de moteurs supraconducteurs, Thèse de doctorat de l'Université Henri Poincaré, Nancy I.

[25] Stavrev, S. (2002).Modelling of high temperaturesuperconductors for AC power applications, Thèse de doctorat, école polytechnique fédérale de Lausanne (EPFL).

[26] BEN ALIA, Kh. (2013). ETUDE DES SYSTEMES DE GUIDAGE MAGNETIQUE A BASE DE SUPRACONDUCTEUR HTc, Thèse de doctorat, Université Mohamed Khider de Biskra.

[27] Yannick, C. (2007). Limiteur Supraconducteur de Courant Continu. Thèse de Doctorat, Institut National Polytechnique de Grenoble, 13 décembre.

[28] BAIXIRAS, J. (1998). Les Supraconducteurs Applications à l'électronique et à l'électrotechnique, CNRS EDITIONS France.

[29] KEBBAB, N. (2007). Les Supraconducteurs, Modèles et Applications, Mémoire de Magister, Université de Batna.

[30] NEMDILI, S. (2013). Modélisation et Simulation du Limiteur de Courant Supraconducteur, Thèse de Doctorat, Université Ferhat Abbas Sétif-1.

[31] KLUTSCH, I. (2003). Modélisation des supraconducteurs et mesures, Thèse de Doctorat, Institut National Polytechnique de Grenoble.

[32] Source : B. Gamble, G. Snitchler, T. MacDonald. Full Power Test of a 36.5 MW HTS Propulsion Motor.

[33] BELHAMDI, S. (2021). Modélisation et simulation des systèmes électromécanique. » Cours M2/S3/EM, Université Mohamed Boudiaf M'sila.

[34] Charrier, A. (2006). Propriétés de transport sous contrainte mécanique des conducteurs

[35] Pascal, F. (2003). Conceptual design of 100 MVA superconducting autotransformers. INIST-CNRS

Wang, and C. W. Chu, Phys. Rev. Lett., 58, (1987) 908-910.

[36] MARAF, H., NECIB, Zaineb. (2018). Analyse de L'énergie Dissipative Dans Les Limiteurs de Courant Inductif Pour Les Systèmes D'énergie, Mémoire de Master, Université de KasdiMerbah Ouargla.

[37] ABDESSEMED, R. (2011). Modélisation et simulation des machines électriques, Livre.

[38] Rouahna, F. (2012). Calcul Analytique des Pertes dans les Matériaux Supraconducteurs à Haute Température Critique (SHTc), Mémoire de Master, Université de Biskra,.

[39] Mangin, Ph., KAHN, R. (2017). Matériaux supraconducteurs. EDP Sciences.

[40] BLMILOUD, R. (2022). Commande par linéarisation entré/sortie de la MAS, mémoire de master, Université des Sciences et de la Technologie Mohamed El Bachir El Ibrahimi Bordj Bou arreridj.

[41] Valentin Donnier-Valentin. Contribution à l'étude des transformateurs supraconducteurs. Sciences de l'ingénieur [physics]. Institut National Polytechnique de Grenoble - INPG, 2001. Français. ⟨NNT :⟩. ⟨tel-00597717⟩

[42] Samir, A., &Chafaa, A. L. (2013). *Dimensionnement et calcul de courant de court-circuit d'un transformateur triphasé 100 KVA, 30KV/0.4 KV* (Doctoral dissertation, Université Mouloud Mammeri).

[43] Kothari, D. P., & Nagrath, I. J. (2010). *Modern Power System Analysis* (4th ed.). McGraw-Hill Education.

[44] Wildi, T. (2006). *Electrical Machines, Drives and Power Systems* (6th ed.). Pearson Education.

[45] Gonen, T. (2014). *Electric Power Distribution Engineering* (3rd ed.). CRC Press.

[46] Chapman, S. J. (2012). Electric Machinery Fundamentals (5th ed.). McGraw-Hill.

[47] Sen, P. C. (1997). Principles of Electric Machines and Power Electronics. John Wiley & Sons.

[48] Malozemoff, A. P., et al. (2005). *Superconducting Power Equipment: Technology Watch 2005*. EPRI Report 1011676.

[49] Zhang, M., et al. (2010). "Design and analysis of high temperature superconducting autotransformer for power grid applications." *IEEE Transactions on Applied Superconductivity*, 20(3), 1345–1348.

[50] Hoshino, T., et al. (2014). "Development of 22 kV-class superconducting autotransformer." *Physica C: Superconductivity and its Applications*, 484, 43–47.

[51] **Larbalestier**, **D. C**., et al. (2001). "High-Tc superconducting materials for electric power applications." *Nature*, 414(6861), 368–377.